Performance Analysis of SWIPT-Enabled Cooperative NOMA Networks for 5G and Beyond Wireless Communications

M.Tech. Thesis

By

Kalla Satya Ganapathi Kiran

DISCIPLINE OF ELECTRICAL ENGINEERING

INDIAN INSTITUTE OF TECHNOLOGY INDORE

JUNE 2021

Performance Analysis of SWIPT-Enabled Cooperative NOMA Networks for 5G and Beyond Wireless Communications

A THESIS

Submitted in partial fulfillment of the requirements for the award of the degree

of

Master of Technology

by

Kalla Satya Ganapathi Kiran

DISCIPLINE OF ELECTRICAL ENGINEERING

INDIAN INSTITUTE OF TECHNOLOGY INDORE

JUNE 2021

INDIAN INSTITUTE OF TECHNOLOGY INDORE

CANDIDATE'S DECLARATION

I hereby certify that the work which is being presented in the thesis entitled **Performance Analysis of SWIPT-Enabled Cooperative NOMA Networks for 5G and Beyond Wireless Communications** in the partial fulfillment of the requirements for the award of the degree of **MASTER OF TECHNOLOGY** and submitted in the **DISCIPLINE OF ELECTRICAL ENGINEERING, Indian Institute of Technology Indore**, is an authentic record of my own work carried out during the time period from July 2019 to June 2021 of M.Tech. under the supervision of Dr. Swaminathan Ramabadran, Assistant Professor, Indian Institute of Technology Indore.

The matter presented in this thesis has not been submitted by me for the award of any other degree of this or any other institute.

Ganapathi Kiran 7/6/21

Signature of the student with date
(KALLA SATYA GANAPATHI KIRAN)

This is to certify that the above statement made by the candidate is correct to the best of my/our knowledge.

07/06/2021
Signature of the Supervisor of
M.Tech. thesis (with date)
(Dr. SWAMINATHAN RAMABADRAN)

KALLA SATYA GANAPATHI KIRAN has successfully given his M.Tech. Oral Examination held on **7th June 2021**.

Signature(s) of Supervisor(s) of M.Tech. thesis
Date:07/06/2021

Convener, DPGC
Date: 07/06/2021

Signature of PSPC Member #1
Date: 7-06-2021

Signature of PSPC Member #2
Date: 7/6/2021

Acknowledgments

Firstly, I would like to express my sincere gratitude to my supervisor Dr. Swaminathan Ramabadran for his continuous support and valuable guidance. His guidance helped me in throughout my work. I have been able to push myself beyond my expectations with his excellent supervision and encouragement.

I would like to thank my PSPC members Dr. Prabhat Kumar Upadhyay and Dr. I.A.Palani for their insightful comments and suggestions towards my research.

I sincerely acknowledge IIT Indore and MHRD for supporting my M.Tech. by providing lab facilities and TA scholarship, respectively.

Last but not least, my work would not have been possible without the encouragement of my parents, whose tremendous support helped me stay positive and overcome the worst of hurdles. To them, I will forever be grateful.

Abstract

Wireless mobile communication and its applications have become a crucial part of our daily lives. With the increasing number of wireless devices, the number of users, and massive data traffic, the significant challenges for today's Fourth-Generation (4G) wireless communication system are the effective utilization of Radio Frequency (RF) spectrum and energy efficiency. Also, it is to be noted that the expected data rates for Fifth-Generation (5G) and beyond communication cannot be achieved using 4G technologies. This led to the development of various new technologies for 5G and beyond wireless communication. Three of the key technologies involved in 5G and beyond are Non-Orthogonal Multiple Access (NOMA), cooperative communication, and RF energy harvesting.

The principal reason for using NOMA in 5G and beyond communication is its capability to serve multiple users using the same time and frequency resources. Two main techniques involved in NOMA are power-domain and code-domain. Power-domain in NOMA attains multiplexing in the power domain, whereas code-domain in NOMA attains multiplexing in the code domain. NOMA dominates typical Orthogonal Multiple Access (OMA) in terms of various aspects like spectral efficiency, connectivity, latency, and fairness. Cooperative NOMA is an extended version of NOMA, which incorporates multiple or single relays into the NOMA networks to improve reliability. Since we are moving towards the design of advanced communication receivers for high data rate applications, the power consumption of wireless devices has become an important issue.

Further, successive interference cancellation (SIC) technique involved in NOMA and complex signal processing techniques will quickly drain the battery life. Hence, to solve the problem of high energy consumption in 5G and beyond wireless systems, RF energy harvesting becomes a promising technology. Conventional energy harvesting techniques using solar power, wind energy, etc., are not reliable. Thus, non-conventional energy harvesting techniques such as Wireless Power Transfer (WPT) and Simultaneous Wireless Information and Power Transfer (SWIPT) will act as a solution. In WPT, the energy from powerful RF sources such as base stations, dedicated access points, etc., can be harvested to power individual wireless nodes. Further, SWIPT enables the wireless nodes to harvest the energy from incoming RF signals using time switching or power splitting techniques

and transmit information using harvested energy. In a nutshell, cooperative NOMA and RF energy harvesting together will serve as promising candidates for 5G and beyond wireless communication.

In our work, the performance analysis of cooperative NOMA networks with and without RF energy harvesting has been investigated over Rayleigh fading channel. We have derived mathematical expressions for performance metrics such as outage probability, system throughput, and ergodic capacity. The derived performance metrics have been validated using Monte-Carlo simulations. Further, the performance of the proposed system models have also analyzed for the cases with imperfect channel state information (CSI) and SIC, which exist in practical scenarios. Finally, various interesting inferences have been reported using the obtained performance metrics.

Contents

List of Figures

Chapter 1

Introduction

1.1 Introduction

Non-Orthogonal Multiple Access (NOMA) has been recognized as a promising multiple access method for the Fifth-Generation (5G) networks due to its higher spectral efficiency and massive connectivity. NOMA is broadly classified into two types: Power Domain (PD) NOMA and code domain NOMA. Here our work is in the direction of PD-NOMA. In PD-NOMA, multiple users are served using the same time, frequency resource blocks but with different power allocation coefficients, i.e., users with better channel conditions are assigned lower power coefficient values, whereas users with poor channel conditions are assigned higher power coefficient values. This thesis will hereafter refer to PD-NOMA as just NOMA. NOMA employs two techniques, namely superposition coding and Successive Interference Cancellation (SIC) at transmitter and receiver, respectively. At the transmitter, multiple users are multiplexed in the power domain using superposition coding. At the receiver, multiple users are demultiplexed using SIC. SIC is an iterative algorithm, where data corresponded to each user is decoded based on the decreasing order of power coefficients allocated to each user, i.e., data corresponds to a user who is allocated with a high power coefficient is decoded first. Then data corresponding to a user who is allocated with the next highest power coefficient is decoded. This process is continued until information corresponding to all users is decoded. Unlike NOMA, Orthogonal Multiple Access (OMA) techniques, such as Frequency Division Multiple Access (FDMA), Time Division Multiple Access (TDMA), Code Division Multiple Access (CDMA), Orthogonal Frequency Division Multiple Access (OFDMA), serve a single user in each orthogonal resource block. These OMA techniques are spectral inefficient compared with the NOMA [5].

In cooperative communication, multiple relays or a single relay are employed between transmitter and receiver. Here in the cooperative communication, apart from the base station, relays also will forward the information to the receiver. In cooperation communication, the information is transmitted in two phases: the base station transmits information to the relay in the first phase. In the second phase, relay forwards information to the receiver. There are two modes of operation at the relay: half-duplex (HD) and full-duplex (FD). Two orthogonal time slots or frequency bands are employed for data transmission and reception in HD mode. Simultaneous transmission and reception on the same frequency band and at the same time is possible in FD mode. In cooperative communication networks along with the base station, the relay node also will transmit the signal to the mobile users. So, mobile users receive the signal from both the base station as well as from the relay. Due to this cooperative communication, diversity gain can be achieved without incorporating multiple antennas at the receiver, and also coverage area of the base station is extended. Integrating NOMA with cooperative communication has several advantages such as reliability, extension of coverage area, and improved diversity gain [4]. So, incorporating NOMA with cooperative communication would be a promising technology for 5G and beyond communication.

Using the strong user as a relay, cooperative NOMA can successfully assist the user with weak channel conditions. However, this user may not want to engage in relaying because it would drain the battery quickly and limit its life. Radio Frequency (RF) energy harvesting is a promising candidate to solve energy consumption issues. With Simultaneous Wireless Information and Power Transfer (SWIPT), the strong user can harvest energy from the incoming RF signals transmitted by the base station and use it to power the relay transmission. As a result, the strong user will have a motive to relay information to the weak user, and the weak user will be able to assisted by the strong user [5]. So, integrating SWIPT with cooperative NOMA would be a promising candidate for 5G and beyond communication.

1.2 Literature Review

Recently, many research works have been done by integrating NOMA with various technologies. Authors in [2] have made a performance comparison between NOMA and OMA for both uplink and downlink scenarios. In terms of sum rate, the NOMA exceeds the OMA in [2]. Further, authors in [2] have investigated Multiple Input Multiple Output (MIMO) NOMA and it is proved that MIMO-NOMA exceeds NOMA in terms of both outage probability and sum rate. For cooperative NOMA systems with finite time slots, a two-stage superposed transmission mechanism is proposed in [7]. Conventional cooperative NOMA (CCN) networks suffer from low spectral efficiency due to a half-duplex limitation. To inscribe this problem, the authors in [12], [19] proposed an incremental cooperative NOMA (ICN) protocol in a downlink scenario and they derived outage probability and system throughput expressions over Rayleigh fading channels. Further, they also demonstrated that the proposed ICN protocol exceeds the CCN protocol. The authors of [14] proposed three cooperative relaying schemes to improve the outage performance for the two far users in the presence of both direct and relay links.

Incorporating multiple relays in a dual-hop cooperative NOMA system provides a significant performance improvement. Two typical relay selection schemes are examined in dual-hop cooperative networks: opportunistic relay selection (ORS) [3] and partial relay selection (PRS) [11]. The PRS technique considers channel state information (CSI) between source and relay links or between the relay and mobile users links for relay selection. The ORS method considers CSI between source and relay links, as well as between relay and mobile users for relay selection. In [11], the authors investigated the outage performance of NOMA with PRS scheme for AF relay systems. RF signal energy harvesting has recently drawn significant attention in wireless communication networks to increase battery lifetime at the wireless sensor nodes, mobile users, and relay [15]. In [15], the authors have considered AF relaying network. Energy is harvested from the received RF signal by an energy-constrained relay node, which is then used to send the base station information to the receiver. In [21], the authors have proposed the SWIPT NOMA networks. Here, the near user acts as an FD mode energy harvesting relay node to aid transmission from source node to far user. To achieve ideal values of power allocation factor and power splitting ratio, an alternative optimization-based approach is proposed [21]. Analysis of NOMA networks having non-linear energy harvesting is carried out in [18], [20], [9]. In a practical scenario, imperfect CSI and imperfect SIC exist in the system. The effects of inaccurate CSI information in an energy harvesting cooperative NOMA system with a source, two users, and an energy harvesting relay are explored in [6]. In [16], authors investigated the performance of cooperative NOMA networks under PRS scheme with outdated CSI. The impact of channel correlation coefficient, relay selection mode, and relay position on system performance has been shown in [16].

The authors in [22] investigated NOMA systems where SIC is applied to both legitimate users and eavesdroppers. Furthermore, to alleviate the SIC error produced by imperfect SIC, a power allocation method is devised for legitimate users [22]. Unlike the SWIPT-enabled cooperative NOMA networks, the research works in [13] considered the SWIPT-enabled cooperative NOMA networks with imperfect CSI and SIC. Performance of cooperative NOMA system with imperfect SIC and CSI is investigated in [1], [10]. The impact of residual hardware impairments, channel estimate errors, and SIC on SWIPT aided cooperative NOMA system over Nakagami-m channels is explored in [13] and closed-form expressions for outage probability and ergodic sum rate are determined. In addition, an asymptotic outage probability analysis is performed. The results reveal that owing to channel estimate problems, the outage probability has an error floor. Furthermore, channel estimate errors have a greater influence on system the performance than residual hardware impairments.

1.3 Motivations and Contributions

1.3.1 Chapter 2

The motivations behind the work in Chapter 2 are summarized as follows:

- The performance of cooperative NOMA with PRS scheme for DF relaying in the presence of both direct link and relay link has not been investigated in the existing literature to the best of our knowledge.
- In particular, the performance analysis in [11] was reported only for the AF relaying. Therefore, there is a need to analyze the performance of the DF relaying.

The contributions of the work in Chapter 2 are summarized as follows:

- The closed-form expressions for performance metrics such as outage probability, ergodic capacity, and overall system throughput of the proposed system model are derived.
- The Monte Carlo simulations are also carried out to validate the derived closed-form expressions.

1.3.2 Chapter 3

The motivations behind the work in Chapter 3 are summarized as follows:

- The existing literature lack in deriving the exact outage probability expression for the SWIPT-enabled cooperative NOMA system over Rayleigh fading channels. Furthermore, most of the works in the multi-relay scenario are limited to AF or DF relaying without a direct link.
- In particular, the outage probability analysis for the SWIPT-enabled cooperative NOMA system over Rayleigh fading channels in [15], [17] are restricted to asymptotic outage probability expressions only.
- There is a need to derive the closed-form expressions for the outage probability in order to perform exact outage probability analysis.

The contributions of the work in Chapter 3 are summarized as follows:

- The exact closed-form outage probability expressions are derived for the proposed system over Rayleigh fading channels.
- In addition, the expressions of ergodic capacity, overall system throughput, and energy efficiency are also derived.
- The diversity order analysis is carried out by deriving the asymptotic outage probability expressions.
- Finally, Monte Carlo simulations are performed to validate the derived performance metrics.

1.3.3 Chapter 4

The motivations behind the work in Chapter 4 are summarized as follows:

- SWIPT-enabled cooperative NOMA system achieves spectral efficiency, energy efficiency, reliability. This system achieves full diversity order if there is perfect CSI. However, perfect CSI is not possible in real-time scenarios.
- The existing literature lacks performance analysis of SWIPT-enabled cooperative NOMA systen with imperfect CSI and SIC in the presence of both the direct link and the relay link.

The contributions of the work in Chapter 2 are summarized as follows:

- The closed-form expressions for performance metrics such as outage probability, ergodic capacity, and overall system throughput of the proposed system model are derived.
- The Monte Carlo simulations are also carried out to validate the derived closed-form expressions.

1.4 Organization of the Thesis

The rest of this thesis is organized as follows: In Chapter 2, the system model of PRS NOMA for DF relay networks is discussed. Further, in chapter 3, the performance analysis of the SWIPT-enabled cooperative NOMA system is carried out. Chapter 4 shows the performance analysis of the SWIPT-enabled cooperative NOMA system with imperfect CSI and SIC. Finally, Chapter 5 includes the conclusion and scope of the future work of this thesis.

Chapter 2

Performance Analysis of NOMA with Partial Relay Selection for DF Relay Networks

2.1 Introduction

This chapter describes a downlink cooperative NOMA system model. We proposed a system model of NOMA with Partial Relay Selection for DF Relay Networks. In the proposed system model, we employed one base station, multiple relays, two mobile users. Further, we assume all receiver nodes know the full CSI of all the links. Out of multiple relays, one is selected based on the relay selection scheme. Here, PRS is considered in our work. In the PRS scheme, only CSI between source-to-relay links are required. One relay is selected out of multiple relays based on the instantaneous signal-to-noise ratio (SNR) between source-to-relay links. Receiver nodes receive the signal from the base station and from the relay in two phases. Out of two received signals, one signal is considered. So, diversity combining is to be employed at receiver nodes. There are various kinds of diversity combining techniques such as selection combining, switched combining, maximum-ratio combining, equal-gain combining. Here in our work, we have considered selection combining diversity technique, which is the simplest and the least complex among all the other techniques. In the selection combining technique, out of two received signals at the receiver node, the received signal which is having maximum signal-to-interference-plus-noise-ratio (SINR) is considered. The performance of this proposed system is analyzed by deriving the exact outage probability, ergodic capacity expressions, and overall system throughput over Rayleigh fading channels.

2.2 Organisation of Chapter

The rest of the chapter is organized as follows: The system model for a Cooperative NOMA system has been discussed in Section 2.3. Section 2.4 provides the closed-form expressions for outage probability and ergodic capacity of both mobile users over Rayleigh fading channels. Furthermore, Numerical results and inferences are given in Section 2.5. Finally, the concluding remarks are given in Section 2.6.

2.3 System Model

Let us consider a downlink cooperative NOMA system model as shown in Figure 2.1, where a base station (BS) S intends to transmit the signal to two mobile users D_1, D_2 with the help of a single DF relay, which is selected out of K number of relays based on PRS scheme. Here out of K relays, one relay is selected based on the instantaneous SNR between S $\rightarrow R_k$ links, Where, $k = 1, 2, ...K$. Here the data transmission takes place in two phases, and we assume symbol by symbol transmission. The relay employs HD mode and all nodes in the network are equipped with a single antenna. Let $h_{i,j}$ represents the independent Rayleigh fading channel coefficient between nodes i and j with variance $\Omega_{i,j}$, Where, i$\neq$j, i $\in${S,R}, j $\in${R_k,D}. The relation between $\Omega_{i,j}$ and the normalized distance between nodes is $\Omega_{i,j} = d_{i,j}^{-n_p}$, where, $d_{i,j}$ is normalised distance between nodes, n_p is path-loss exponent. At the beginning of the transmission, the source node selects one relay based on the channel state information.

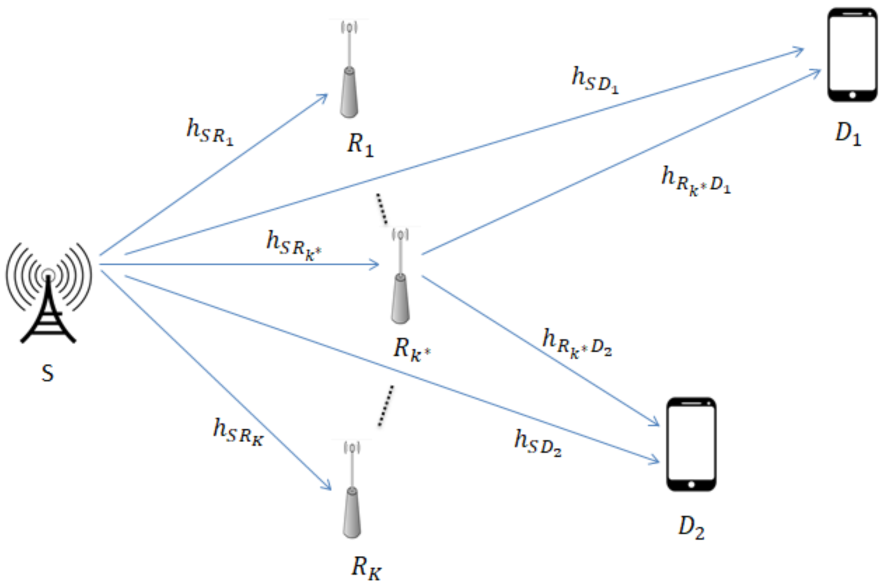

Figure 2.1: System Model

The random variables W_i, X_k, Y_{ik} represents instantaneous SNR of links $S \rightarrow D_i$, $S \rightarrow R_k$, $R_k \rightarrow D_i$, respectively, where, random variables W_i, X_k, Y_{ik} are given as follows:

$$W_i = \rho_s |h_{SD_i}|^2 = \gamma_{SD_i} \tag{2.1}$$

$$X_k = \rho_s |h_{SR_k}|^2 = \gamma_{SR_k} \tag{2.2}$$

$$Y_{ik} = \rho_s |h_{R_k D_i}|^2 = \gamma_{R_k D_i} \tag{2.3}$$

The cumulative distributive functions (CDFs) of random variables W_i, X_k, Y_{ik} are given by

$$F_{W_i}(w_i) = 1 - \ exp\left(\frac{-w_i}{\rho_s \Omega_{SD_i}}\right) \tag{2.4}$$

$$F_{X_k}(x_k) = 1 - \ exp\left(\frac{-x_k}{\rho_s \Omega_{SR_k}}\right) \tag{2.5}$$

$$F_{Y_{ik}}(y_{ik}) = 1 - \ exp\left(\frac{-y_{ik}}{\rho_s \Omega_{R_k D_i}}\right) \tag{2.6}$$

Out of multiple relays, one relay is selected, and that chosen relay will decode the signal received from S in the first phase and then forward the decoded signal to both the users in the second phase. The PRS strategy is employed to select relay based on the instantaneous SNR between S$\rightarrow R_k$. Let the selected relay index is k^*, and its respective instantaneous SNR is obtained as follows:

$$k^* = arg \, {}^{\max}_{k=1,....K} \ X_k \tag{2.7}$$

$$X_{k^*} = {}^{\max}_{k=1,....K} \ \ X_k \tag{2.8}$$

The CDF of the selected relay k^* is

$$F_{X_{k^*}}(x_{k^*}) = P\left(X_{k^*} < x_{k^*}\right) \tag{2.9}$$

$$F_{X_{k^*}}(x_{k^*}) = P\left(\max\left(X_1, X_2, ...X_k\right) < x_{k^*}\right) \tag{2.10}$$

$$F_{X_{k^*}}(x_{k^*}) = P\left(X_1 < x, X_2 < x, ...X_k < x_{k^*}\right) \tag{2.11}$$

$$F_{X_{k^*}}(x_{k^*}) = P\left(X_1 < x_{k^*}\right) P\left(X_2 < x_{k^*}\right) .... \tag{2.12}$$

After substituting (2.5) in (2.12), the CDF of selected relay is given as follows

$$F_{X_{k^*}}(x_{k^*}) = \left[1 - \ \exp\left(\frac{-x_{k^*}}{\rho_s \Omega_{SR_1}}\right)\right]\left[1 - \ \exp\left(\frac{-x_{k^*}}{\rho_s \Omega_{SR_2}}\right)\right] .... \tag{2.13}$$

Let $\Omega_{SR_1} = \Omega_{SR_2} = ...\Omega_{SR_K}$

So, now CDF of the selected relay k^* is rewirtten as follows

$$F_{X_{k^*}}(x_{k^*}) = \left[1 - \ \exp\left(\frac{-x_{k^*}}{\rho_s \Omega_{SR_{k^*}}}\right)\right]^K \tag{2.14}$$

$$F_{X_{k^*}}(x_{k^*}) = \sum_{k=0}^{k=K} \binom{K}{k} (-1)^k \exp\left(\frac{-x_{k^*}k}{\rho_s \Omega_{SR_{k^*}}}\right) \tag{2.15}$$

$$F_{X_{k^*}}(x_{k^*}) = 1 - \sum_{k=1}^{k=K} \binom{K}{k} (-1)^{k-1} \exp\left(\frac{-x_{k^*}k}{\rho_s \Omega_{SR_{k^*}}}\right) \tag{2.16}$$

First Phase:

The received signals at both mobile users D_1, D_2 are given by

$$y_{D_1} = h_{SD_1}(\sqrt{a_1 p_s} x_1 + \sqrt{a_2 p_s} x_2) + n_{D_1} \tag{2.17}$$

$$y_{D_2} = h_{SD_2}(\sqrt{a_1 p_s} x_1 + \sqrt{a_2 p_s} x_2) + n_{D_2} \tag{2.18}$$

where n_{D_1} and n_{D_2} denote the additive white gaussian noise (AWGN) with zero mean and variance σ^2, h_{SD_1} and h_{SD_2} are the fading channel coefficients, a_i denotes power coefficient for symbol x_i, i=1,2, p_s is transmission power at the S. As user1 is far away from the base station compared to user2 so, $a_1 \geq a_2$.

The received SINR at D_1 to detect its symbol x_1 is given by

$$\gamma_1 = \frac{a_1 p_s |h_{SD_1}|^2}{a_2 p_s |h_{SD_1}|^2 + \sigma^2} \tag{2.19}$$

$$\gamma_1 = \frac{a_1 W_1}{a_2 W_1 + 1} \tag{2.20}$$

where, $\rho_s = \frac{p_s}{\sigma^2}$ represents the average SNR.

The received SINR at D_2 to detect symbol x_1 is given by

$$\gamma_{1,2} = \frac{a_1 W_2}{a_2 W_2 + 1} \tag{2.21}$$

The received SINR at D_2 to detect its symbol x_2 after SIC is given by

$$\gamma_2 = a_2 W_2 \tag{2.22}$$

The received signal at selected relay k^* from S is

$$y_{R_{k^*}} = h_{SR_{k^*}}(\sqrt{a_1 p_s} x_1 + \sqrt{a_2 p_s} x_2) + n_{R_{k^*}} \tag{2.23}$$

where, $n_{R_{k^*}}$ represents AWGN at relay k^* having zero mean and variance σ^2

The received SINR at R_{k^*} to detect symbol x_1 is given by

$$\gamma_{R,1} = \frac{a_1 X_{k^*}}{a_2 X_{k^*} + 1} \tag{2.24}$$

The received SINR at R_{k^*} to detect symbol x_2 after SIC is given by

$$\gamma_{R,2} = a_2 X_{k^*} \tag{2.25}$$

Second phase: The received signal at D_1 and D_2 in the second phase can be expressed as

$$y_1^{DF} = \sqrt{a_1 p_s} x_1 h_{R_{k^*}D_1} + \sqrt{a_2 p_s} x_2 h_{R_{k^*}D_1} + n_1 \tag{2.26}$$

$$y_2^{DF} = \sqrt{a_1 p_s} x_1 h_{R_{k^*}D_2} + \sqrt{a_2 p_s} x_2 h_{R_{k^*}D_2} + n_2 \tag{2.27}$$

where n_1 and n_2 represent the AWGN at D_1 and D_2 , respectively, with zero mean and variance σ^2 , transmission power at relay is p_r and we assume $p_r = p_s$. The received SINR at D_1 to detect its symbol x_1 is given by

$$\gamma_1^{DF} = \frac{a_1 Y_{1k^*}}{a_2 Y_{1k^*} + 1} \tag{2.28}$$

The received SINR at D_2 to detect symbol x_1 is given by

$$\gamma_{1,2}^{DF} = \frac{a_1 Y_{2k^*}}{a_2 Y_{2k^*} + 1} \tag{2.29}$$

The received SINR at D_2 to detect its symbol x_2 after SIC is given by

$$\gamma_{1,2}^{DF} = a_2 Y_{2k^*} \tag{2.30}$$

2.4 Performance Analysis

2.4.1 Outage Probability Analysis of User1

The outage probability of the D_1 is given by

$$P_1 = P\left(\max\left(\gamma_{SD_1}, \gamma_{R_{k^*}D_1}\right) < \gamma_{th}\right) \tag{2.31}$$

where γ_{th} is SINR threshold

$$= P\left(\gamma_{SD_1} < \gamma_{th} \cap \gamma_{R_{k^*}D_1} < \gamma_{th}\right) \tag{2.32}$$

$$= P\left(\gamma_{SD_1} < \gamma_{th}\right) P\left(\gamma_{R_{k^*}D_1} < \gamma_{th}\right) \tag{2.33}$$

$$P_1 = P\left(\gamma_1 < \gamma_{th}\right) P\left(\gamma_{R,1} < \gamma_{th} \cup \gamma_{R,2} < \gamma_{th} \cup \gamma_1^{DF} < \gamma_{th}\right) \tag{2.34}$$

After simplifying the above equation, we can rewrite it as follows

$$P_1 = P\left(\gamma_1 < \gamma_{th}\right)\left(1 - P\left(\gamma_{R,1} > \gamma_{th} \cap \gamma_{R,2} > \gamma_{th} \cap \gamma_1^{DF} > \gamma_{th}\right)\right) \tag{2.35}$$

After, substituting (2.20), (2.24), (2.25), (2.28) in (2.35), we get

$$P_1 = P\left(W_1 < \phi_1\right)\left(1 - P\left(X_k* > \phi_2 \cap Y_{1k^*} > \phi_1\right)\right) \tag{2.36}$$

$$where, \;\; \phi_1 = \frac{\gamma_{th}}{(a_1 - a_2\gamma_{th})}, \;\; \phi_2 = \max\left(\frac{\gamma_{th}}{(a_1 - a_2\gamma_{th})}, \frac{\gamma_{th}}{a_2}\right) \tag{2.37}$$

After, substituting (2.4), (2.16), (2.6), in (2.36), we get

$$P_1 = \left(1 - \exp\left(\frac{-\phi_1}{\rho_s \Omega_{SD_1}}\right)\right)\left(1 - \sum_{k=1}^{k=K}\binom{K}{k}(-1)^{(k-1)}\exp\left(\frac{-\phi_2}{\rho_s \Omega_{SR_{k^*}}}\right)\exp\left(\frac{-\phi_1}{\rho_s \Omega_{R_{k^*}D_1}}\right)\right) \tag{2.38}$$

2.4.2 Outage Probability Analysis of User2

The outage probability of the D_2 is given by

$$P_2 = P\left(\max\left(\gamma_{SD_2}, \gamma_{R_{k^*}D_2}\right) < \gamma_{th}\right) \tag{2.39}$$

$$= P\left(\gamma_{SD_2} < \gamma_{th} \cap \gamma_{R_{k^*}D_2} < \gamma_{th}\right) \tag{2.40}$$

$$= P\left(\gamma_{SD_2} < \gamma_{th}\right) P\left(\gamma_{R_{k^*}D_2} < \gamma_{th}\right) \tag{2.41}$$

After simplifying the above equation, we can rewrite it as follows

$$P_2 = P\left(\gamma_{1,2} < \gamma_{th} \cup \gamma_2 < \gamma_{th}\right) P\left(\gamma_{R,1} < \gamma_{th} \cup \gamma_{R,2} < \gamma_{th} \cup \gamma_{1,2}^{DF} < \gamma_{th} \cup \gamma_2^{DF} < \gamma_{th}\right) \tag{2.42}$$

After simplifying the above equation, it can rewritten follows

$$P_2 = \left(1 - P\left(\gamma_{1,2} > \gamma_{th} \cap \gamma_2 > \gamma_{th}\right)\right)\left(1 - P\left(\gamma_{R,1} > \gamma_{th} \cap \gamma_{R,2} > \gamma_{th} \cap \gamma_{1,2}^{DF} > \gamma_{th} \cap \gamma_2^{DF} > \gamma_{th}\right)\right) \tag{2.43}$$

After, substituting (2.21), (2.22), (2.24), (2.25), (2.29), (2.30) in (2.43), we get

$$P_2 = \left(1 - P\left(W_2 > \phi_2\right)\right)\left(1 - P\left(X_k* > \phi_2 \cap Y_{2k^*} > \phi_2\right)\right) \tag{2.44}$$

After, substituting (2.4), (2.16), (2.6), in (2.44), we get

$$P_2 = \left(1 - \exp\left(\frac{-\phi_2}{\rho_s \Omega_{SD_2}}\right)\right)\left(1 - \sum_{k=1}^{k=K}\binom{K}{k}(-1)^{(k-1)}\exp\left(\frac{-\phi_2}{\rho_s \Omega_{SR_{k^*}}}\right)\exp\left(\frac{-\phi_2}{\rho_s \Omega_{R_{k^*}D_2}}\right)\right) \tag{2.45}$$

2.4.3 Ergodic Capacity Analysis of User1

The ergodic capacity of the user1 is given by

$$C_1 = E\left[\frac{1}{2} log_2\left(1 + Z_1\right)\right] \tag{2.46}$$

Z_1 is a random variabe and $Z_1 = \max\left(\gamma_1, \min\left(\gamma_{R,1}, \gamma_1^{DF}\right)\right)$

$$C_1 = \frac{1}{2\ln(2)}\int_0^\infty \frac{1 - F_{Z_1}(x)}{1 + x} dx \tag{2.47}$$

$$\text{where } F_{Z_1}(x) = P\left(\max\left(\gamma_1, \min\left(\gamma_{R,1}, \gamma_1^{DF}\right)\right) < x\right) \tag{2.48}$$

$$F_{Z_1}(x) = P\left(\gamma_1 < x \cap \min\left(\gamma_{R,1}, \gamma_1^{DF}\right) < x\right) \tag{2.49}$$

After simplifying the above equation, we can rewrite it as follows

$$F_{Z_1}(x) = P\left(\gamma_1 < x\right)\left(1 - P\left(\max\left(\gamma_{R,1}, \gamma_1^{DF}\right) > x\right)\right) \tag{2.50}$$

After, substituting (2.20), (2.24), and (2.28) in (2.50), we get

$$F_{Z_1}(x) = P(W_1 < \mu_1)(1 - P(X_{k^*} > \mu_1) P(Y_{1k^*} > \mu_1)) \tag{2.51}$$

$$\text{where,} \;\; \mu_1 = \frac{x}{(a_1 - a_2 x)} \tag{2.52}$$

After substituting (2.4), (2.16), (2.6) in (2.51), we get

$$F_{Z_1}(x) = \left[1 - \exp\left(\frac{-\mu_1}{\rho_s \Omega_{SD_1}}\right)\right]\left[1 - \sum_{k=1}^{k=K} \binom{K}{k} (-1)^{(k-1)} \exp\left(\frac{-\mu_1 k}{\rho_s \Omega_{SR_{k^*}}}\right) \times \exp\left(\frac{-\mu_1}{\rho_s \Omega_{R_{k^*}D_1}}\right)\right] \tag{2.53}$$

After simplifying the above equation, we can rewrite it as follows

$$F_{Z_1}(x) = \left[1 - \exp\left(\frac{-\mu_1}{\rho_s \Omega_{SD_1}}\right)\right] + \left[\sum_{k=1}^{k=K} \binom{K}{k} (-1)^{(k-1)} \exp\left(\frac{-\mu_1}{\rho_s}\left(\frac{k}{\Omega_{SR_{k^*}}} + \frac{1}{\Omega_{R_{k^*}D_1}}\right)\right) \times \left(1 - \exp\left(\frac{-\mu_1}{\rho_s \Omega_{SD_1}}\right)\right)\right] \tag{2.54}$$

The above equation is valid only if $x < \frac{a_1}{a_2}$

After substituting (2.54) in (2.47), we get

$$C_1 = \frac{1}{2\ln(2)} \int_0^{\frac{a_1}{a_2}} \frac{1 - F_{Z_1}(x)}{1 + x} dx \tag{2.55}$$

The above equation can be re-written as

$$C_1 = \frac{1}{2\ln(2)} \int_0^{\frac{a_1}{a_2}} \frac{\mathscr{B}}{1 + x} dx \tag{2.56}$$

$$\textit{where, } \mathscr{B} = \exp\left(\frac{-\mu_1}{\rho_s \Omega_{SD_1}}\right) - \left[\sum_{k=1}^{k=K} \binom{K}{k} (-1)^{(k-1)} \exp\left(\frac{-\mu_1}{\rho_s}\left(\frac{k}{\Omega_{SR_{k^*}}} + \frac{1}{\Omega_{R_{k^*}D_1}}\right)\right) \times \left(1 - \exp\left(\frac{-\mu_1}{\rho_s \Omega_{SD_1}}\right)\right)\right] \tag{2.57}$$

2.4.4 Ergodic Capacity Analysis of user2

The ergodic capacity of the user2 is given by

$$C_2 = E\left[\frac{1}{2} log_2(1 + Z_2)\right] \tag{2.58}$$

Z_2 is a random variabe and Z_2 = $\max\left(\gamma_2, \min\left(\gamma_{R,2}, \gamma_2^{DF}\right)\right)$

$$C_2 = \frac{1}{2\ln(2)} \int_0^{\infty} \frac{1 - F_{Z_2}(x)}{1 + x} dx \tag{2.59}$$

$$\textit{where } F_{Z_2}(x) = P\left(\max\left(\gamma_2, \min\left(\gamma_{R,2}, \gamma_2^{DF}\right)\right) < x\right) \tag{2.60}$$

$$F_{Z_2}(x) = P\left(\gamma_2 < x \cap \min\left(\gamma_{R,2}, \gamma_2^{DF}\right) < x\right) \tag{2.61}$$

After simplifying the above equation, we can rewrite it as follows

$$F_{Z_2}(x) = P(\gamma_2 < x)\left(1 - P\left(\max\left(\gamma_{R,2}, \gamma_2^{DF}\right) > x\right)\right) \tag{2.62}$$

After, substituting (2.22), (2.25), and (2.30) in (2.62), we get

$$F_{Z_2}(x) = P\left(W_2 < \frac{x}{a_2}\right)\left(1 - P\left(X_{k^*} > \frac{x}{a_2}\right)P\left(Y_{2k^*} > \frac{x}{a_2}\right)\right) \tag{2.63}$$

After, substituting (2.4), (2.16), and (2.6) in (2.63), we get

$$\begin{aligned} F_{Z_2}(x) = \left[1 - \exp\left(\frac{-x}{a_2\rho_s\Omega_{SD_2}}\right)\right]\left[1 - \sum_{k=1}^{k=K}\binom{K}{k}(-1)^{(k-1)}\left[\exp(-x\mu_2)\right.\right. \\ \left.\left. - \exp(-x\mu_3)\right]\right] \end{aligned} \tag{2.64}$$

$$where,\ \ \mu_2 = \frac{k}{a_2\rho_s\Omega_{SR_{k^*}}} + \frac{1}{a_2\rho_s\Omega_{SD_2}},\ \ \mu_3 = \mu_2 + \left(\frac{1}{a_2\rho_s\Omega_{R_{k^*}D_2}}\right) \tag{2.65}$$

After, substituting (2.64) in (2.59), we get

$$C_2 = \frac{1}{2\ln(2)}\left[\int_0^\infty \frac{\exp\left(\frac{-x}{a_2\rho_s\Omega_{SD_2}}\right)}{1+x}dx + \int_0^\infty \frac{\sum_{k=1}^{k=K}\binom{K}{k}(-1)^{(k-1)}\left(\exp(-x\mu_2) - \exp(-x\mu_3)\right)}{1+x}dx\right] \tag{2.66}$$

After simplifying the above equation, we can rewrite it as follows

$$\begin{aligned} C_2 = \frac{1}{2\ln(2)}\left[\left[-\exp\left(\frac{1}{a_2\rho_s\Omega_{SD_2}}\right)Ei\left(\frac{-1}{a_2\rho_s\Omega_{SD_2}}\right)\right] + \left[\sum_{k=1}^{k=K}\binom{K}{k}(-1)^{(k-1)}\right.\right. \\ \left.\left.\times\left[-\exp(\mu_2)Ei(-\mu_2) + \exp(\mu_3)Ei(-\mu_3)\right]\right]\right] \end{aligned} \tag{2.67}$$

where, Ei(.) represents the exponential integral function [8, Eq. (3.352.4)]

2.4.5 Overall System Throughput

The overall system throughput is given by

$$R = (1 - P_1)R_1 + (1 - P_2)R_2 \tag{2.68}$$

where, P_1 and P_2 are obtained from (2.38) and (2.45) respectively. R_1 and R_2 are target rates of user1 and user2 respectively.

2.5 Numerical Results and Discussions

In this section, we will analyze the derived closed-form expressions. We also demonstrate the effects of various parameters on outage probability, overall system throughput, ergodic capacity for the proposed system model. For numerical investigation, we set $a_1 = 0.7$, $a_2 = 0.3$, $\gamma_{th} = 2$ dB, $n_p = 4$, $R_1 = 1.5, R_2 = 1.5$, $\Omega_{SD_1} = (1)^{-4}$, $\Omega_{SD_2} = (0.75)^{-4}$, $\Omega_{SR_{k^*}} = (0.5)^{-4}$, $\Omega_{R_{k^*}D_1} = (0.5)^{-4}$, and $\Omega_{R_{k^*}D_2} = (0.25)^{-4}$

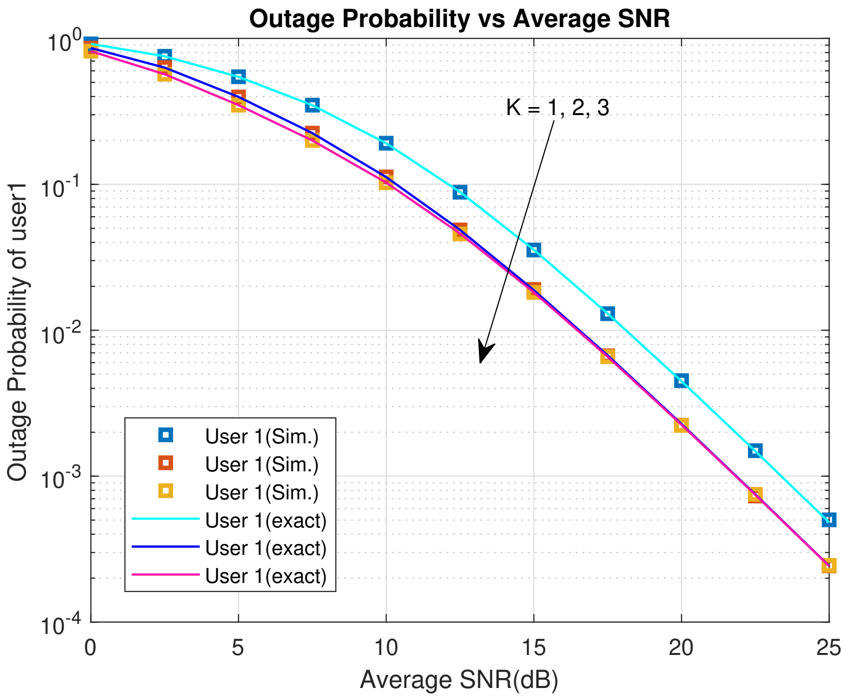

Figure 2.2: Outage Probability vs. Average SNR of user1 for different values of K

Figure 2.2 shows the effect of number of relays in system (K) on the outage probability of the user2. From the plot, we can observe that with the increase in value of K, the outage performance improves. Because if more relays are employed in this system, then the best relay can be selected out of K relays. To achieve the outage probability of 10^{-2}, the SNR required for the system with K=1, K=2, and K=3 are 18 dB, 16.5 dB, 16.5 dB, respectively. So, the SNR gain achieved by the system with K=2, K=3 w.r.t system with K=1 are 2.5 dB, 2.5 dB, respectively. So, it has been inferred that with the increase in value of K above 2, there is no improvement in SNR gain. When SNR increases, the outage probability tends to decrease. It is because as SNR increases, the signal becomes much stronger than the noise.

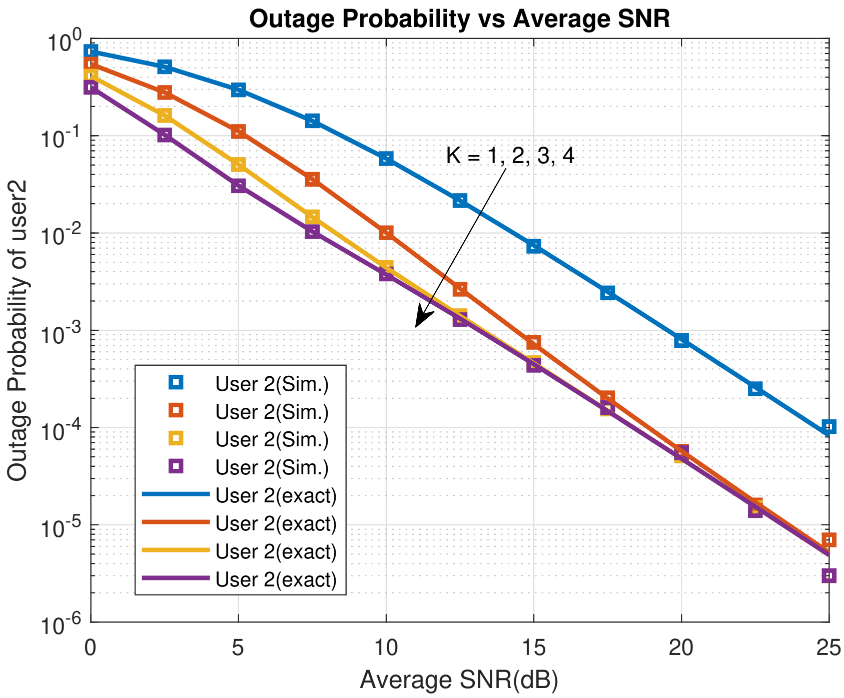

Figure 2.3: Outage Probability vs. Average SNR of user2 for different values of K

Figure 2.3 shows the effect of value of K on the outage probability of the user2. From the plot, we can observe that with the increase in the number of relays, the outage performance improves. Because if more relays are employed in this system model, then the best relay can be selected out of K relays. To achieve the outage probability of 10^{-2}, the SNR required for the system with K=1, K=2, K=3, and K=4 are 14 dB, 10 dB, 8 dB, 7.5 dB, respectively. So, the SNR gain achieved by the system with K=2, K=3, and K=4 w.r.t system with K=1 are 4 dB, 6 dB, 6.5 dB respectively. So, it has been inferred that with the increase in value of K above 3, there is not much improvement in SNR gain.

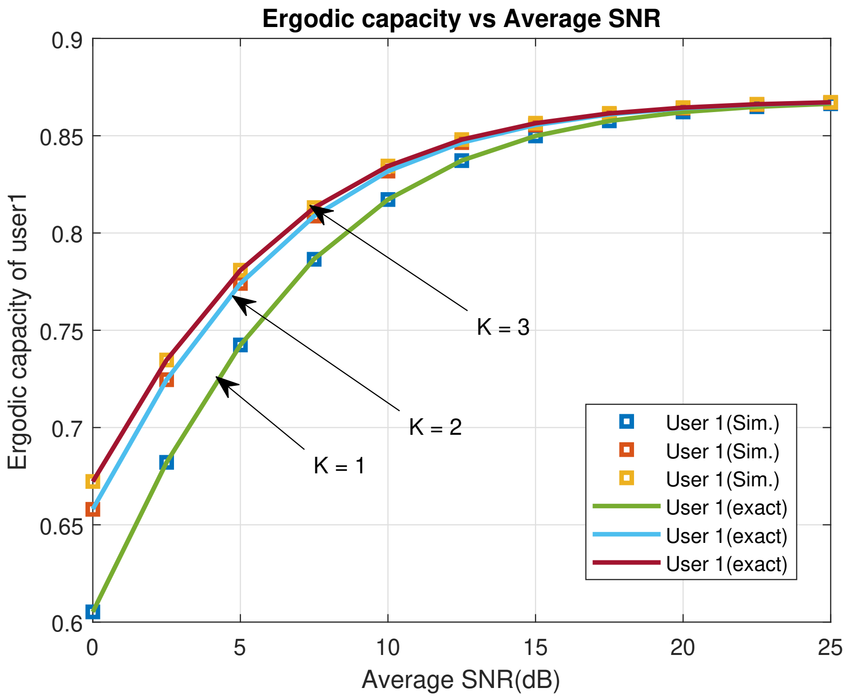

Figure 2.4: Ergodic capacity vs. Average SNR of user1 for different values of K

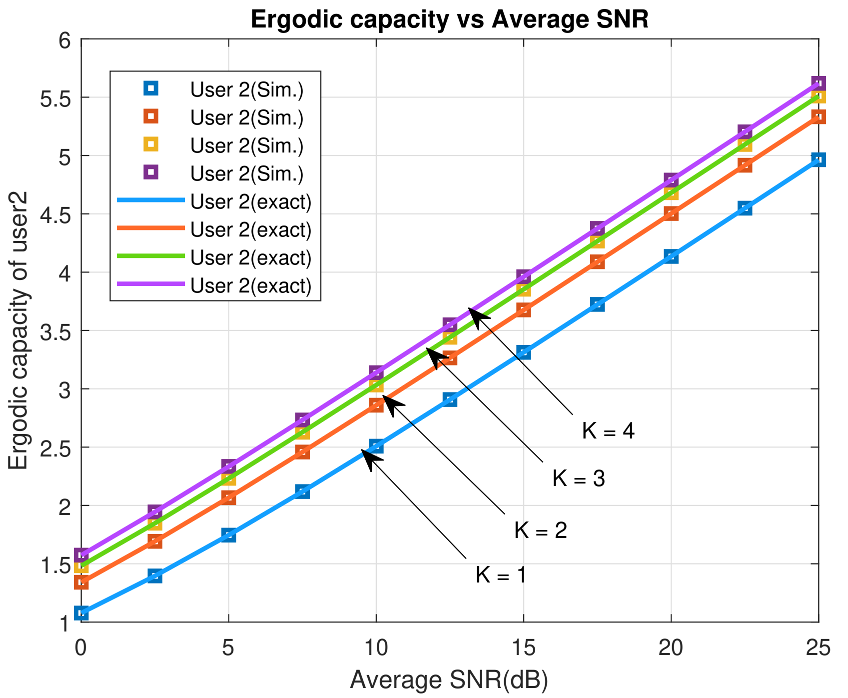

Figure 2.5: Ergodic Capacity vs. Average SNR of user2 for different values of K

Figure 2.4 and 2.5 shows the effect of the number of relays in system on the ergodic capacity of the user1 and user2 respectively. From both figures, we can observe that with the increase in value of K, the ergodic capacity increases slightly. For user1, the ergodic capacity saturates at high SNR. It is because, user1 decodes its signal by considering the user2 signal as noise. For user2, the ergodic capacity increases linearly with SNR. It is because while decoding its signal, the user2 has no interference with the user1 signal.

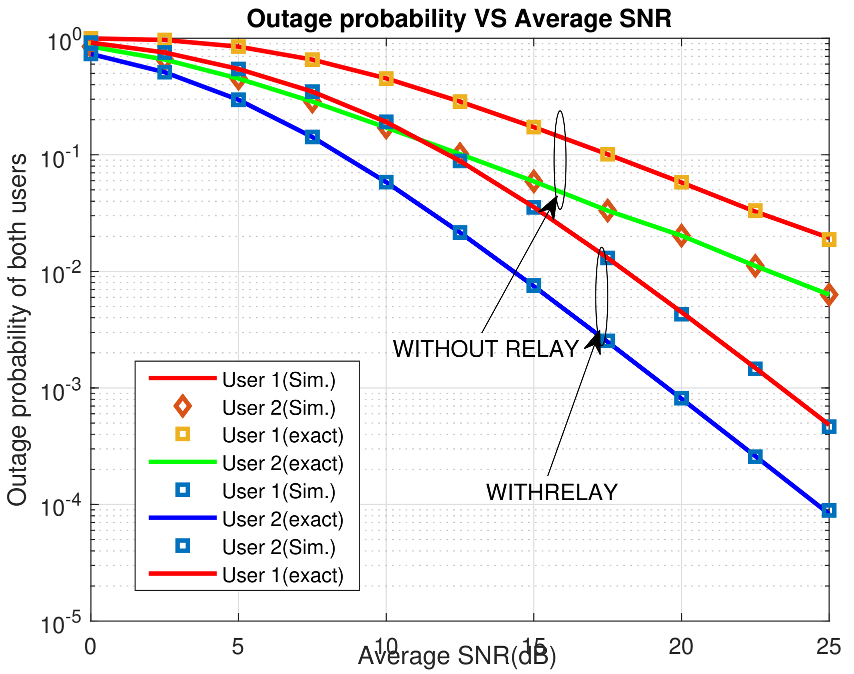

Figure 2.6: Outage Probability vs. Average SNR for system with relay and system without relay

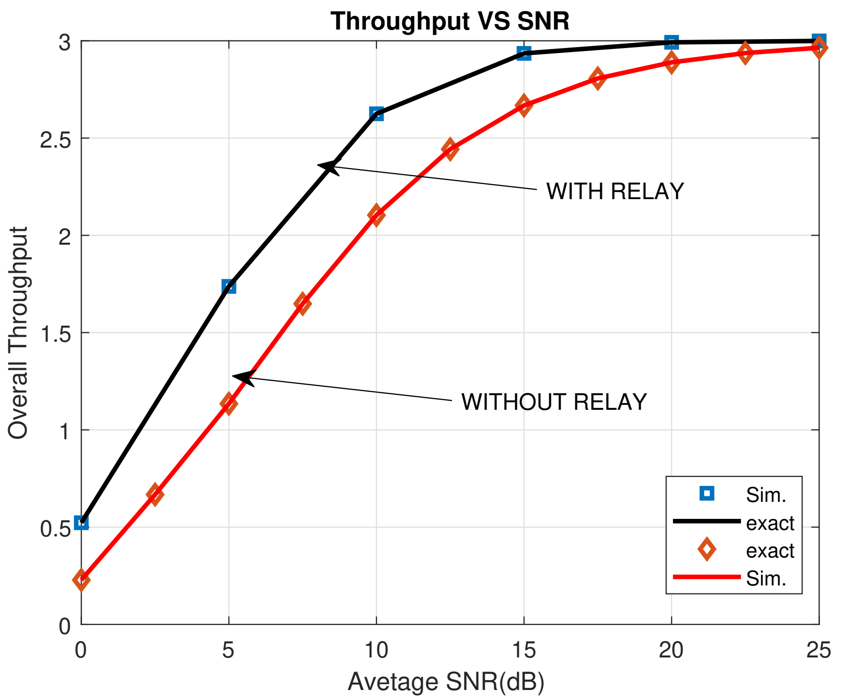

Figure 2.7: Throughput vs. Average SNR for system with relay and system without relay

Figure 2.6 and 2.7 show the impact of the relay on the outage probability and overall system throughput respectively. From both plots, we can observe that system with a relay has better performance than system without a relay in terms of both outage probability and throughput. It has been inferred from Figure 2.6 that to obtain the outage probability of 10^{-2}, SNR required for the system with a relay is 8.5 dB lesser when compared to the system without a relay. From figure 2.7, it is inferred that to obtain throughput of 2.5 bits/sec/Hz, SNR required for the system with a relay is 3.5 dB lesser when compared to the system without a relay. When SNR increases, the throughput tends to increases and saturates at high SNR. It is because, at high SNR, outage probability is almost zero, so throughput will be the sum of target rates of both users.

2.6 Conclusions

In this chapter, the performance analysis of the PRS scheme for the DF-relay-based cooperative NOMA system is carried out by deriving the exact outage probability and ergodic capacity expressions in closed-from over Rayleigh fading channels. Furthermore, closed-form expressions for performance metrics such as outage probability, ergodic capacity, and overall system throughput of the proposed system model are implemented in MATLAB. From simulation results, it is observed that the outage performance of the proposed system model for both users improves with the increase in value of K. Also, outage performance for the system with relay is better than the system without relay, and also, there is improvement in diversity gain for the system with a relay. Further, it is observed that ergodic capacity for user1 saturates at high SNR while ergodic capacity for user2 proportionally increases with SNR. It is inferred from the simulation results that the ergodic capacity of both users increases with an increase in value of K. Finally, the simulated outage probability and ergodic capacity values obtained from Monte Carlo simulations agree well with the theoretical outage probability and ergodic capacity values. Therefore, the derived expressions are validated using simulations as well.

Chapter 3

SWIPT Enabled Cooperative NOMA Networks for 5G and Beyond Wireless Communication Systems

3.1 Introduction

The exact expressions of performance metrics for the downlink cooperative NOMA system model are derived over Rayleigh fading channels in chapter 2. The proposed system model in chapter 2 has achieved reliability enhancement and also spectral enhancement. Energy harvesting has emerged as a promising technology to enhance energy efficiency. To achieve energy enhancement, the energy harvesting technique should be incorporated into the proposed system model. So, in this chapter, we used the SWIPT energy harvesting technique in the proposed downlink cooperative NOMA system. In this chapter, we discuss the SWIPT-enabled cooperative NOMA system model for DF networks. Time switching-based relaying (TSR) protocol is considered in our work. The performance of this proposed system is analyzed by deriving closed-form expressions of outage probability, ergodic capacity, energy efficiency, and overall system throughput over Rayleigh fading channels.

3.2 Organisation of Chapter

The rest of the chapter is organized as follows: The system model for a SWIPT-enabled cooperative NOMA system has been discussed in Section 3.3. Section 3.4 provides the closed-form expressions for the outage probability, ergodic capacity, overall system throughput, and energy efficiency over Rayleigh fading channels. Furthermore, numerical results and inferences are given in Section 3.5.

Finally, the concluding remarks are given in Section 3.6.

3.3 System Model

The communication block diagram with the total block time T for two phases in the TSR protocol is shown in the figure 3.1. The first sub-block of time, i.e., αT, is for energy harvesting, the first half of the remaining block, i.e., $(1-\alpha)$T/2, is for the information transmission between S to selected relay and then the remaining $(1-\alpha)$T/2 is for the information transmission between R_k to D_i. Where, i=1,2. and k = 1,2,...K. Let α, $0 < \alpha < 1$, denote the time allocation ratio. The transmission between source to D_i happens in two phases. In the first phase, the source sends a power multiplexed signal to D_i and the selected relay. Here, the transmission between S and selected relay transmission in the first phase is further divided into two sub-phases: the energy harvesting and decoding phase. In the energy harvesting phase, the selected relay harvest the energy from the received signal from S for sub-block time αT, and it decodes the received signal from S for sub-block time $(1-\alpha)$T/2. In the second phase, selected relay will forward the decoded signal in sub-block time $(1-\alpha)$T/2 to D_i with the harvested energy from S. Both mobile users receive the signal from S and from the selected relay and selection combining is employed at D_i.

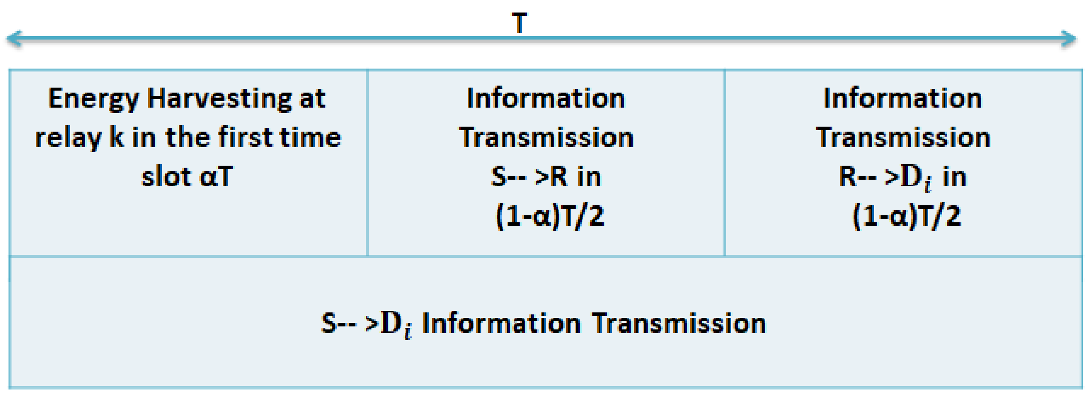

Figure 3.1: Time switching-based relaying protocol of the energy harvesting system

The CDFs of random variables $|h_{SD_i}|^2$, $|h_{SR_k}|^2$, $|h_{R_kD_i}|^2$ are given by

$$F_{|h_{SD_i}|^2}(x) = 1 - \exp\left(\frac{-x}{\Omega_{SD_i}}\right) \tag{3.1}$$

$$F_{|h_{SR_k}|^2}(y) = 1 - \exp\left(\frac{-y}{\Omega_{SR_k}}\right) \tag{3.2}$$

$$F_{|h_{R_kD_i}|^2}(z) = 1 - \exp\left(\frac{-z}{\Omega_{R_kD_i}}\right) \tag{3.3}$$

Out of multiple relays, one relay is selected, and that chosen relay will harvest energy from S, decode the signal received from S and then forward the decoded signal to both users with the harvested energy in the forwarding phase.
The PRS strategy is employed to select relay based on the instantaneous SNR between S$\rightarrow R_k$. Let the selected relay index is k^*, and its respective instantaneous SNR is as follows:

$$k^* = arg \max_{k=1,....K} \ \rho_s |h_{SR_k}|^2 \tag{3.4}$$

$$\rho_s |h_{SR_{k^*}}|^2 = \max_{k=1,....K} \ \rho_s |h_{SR_k}|^2 \tag{3.5}$$

The CDF of the selected relay k^* is

$$F_{|h_{SR_{k^*}}|^2}(x) = P\left(|h_{SR_{k^*}}|^2 < x\right) \tag{3.6}$$

$$F_{|h_{SR_{k^*}}|^2}(x) = P\left(\max\left(|h_{SR_1}|^2, |h_{SR_2}|^2, ...|h_{SR_k}|^2\right) < x_{k^*}\right) \tag{3.7}$$

After simplifying the above equation, we can rewrite it as follows

$$F_{|h_{SR_{k^*}}|^2}(x) = \prod_{k=1}^{K} P\left(|h_{SR_k}|^2 < x\right) \tag{3.8}$$

After, substituting (3.2) in (3.8) the CDF of selected relay is as follows:

$$F_{|h_{SR_{k^*}}|^2}(x) = \prod_{k=1}^{K} \left[1 - \ \exp\left(\frac{-x}{\Omega_{SR_k}}\right)\right] \tag{3.9}$$

Let $\Omega_{SR_1} = \Omega_{SR_2} = ...\Omega_{SR_K}$
So, now CDF of the selected relay k^* is rewritten as follows

$$F_{|h_{SR_{k^*}}|^2}(x) = \left[1 - \ \exp\left(\frac{-x}{\Omega_{SR_{k^*}}}\right)\right]^K \tag{3.10}$$

$$F_{|h_{SR_{k^*}}|^2}(x) = \sum_{k=0}^{k=K} \binom{K}{k} (-1)^k \exp\left(\frac{-xk}{\rho_s \Omega_{SR_{k^*}}}\right) \tag{3.11}$$

$$F_{|h_{SR_{k^*}}|^2}(x) = 1 - \sum_{k=1}^{k=K} \binom{K}{k} (-1)^{k-1} \exp\left(\frac{-xk}{\rho_s \Omega_{SR_{k^*}}}\right) \tag{3.12}$$

In the first phase S transmits the signal to both users and the selected relay and in the second phase selected relay will forward the decoded signal to both users. The transmission between the source and selected relay in the first phase is divided into two more sub-phases called energy harvesting and decoding phases.
First Phase: The Received signals at both mobile users D_1, D_2 are given by

$$y_{D_1} = h_{SD_1}\left(\sqrt{a_1 p_s} x_1 + \sqrt{a_2 p_s} x_2\right) + n_{D_1} \tag{3.13}$$

$$y_{D_2} = h_{SD_2}(\sqrt{a_1 p_s}x_1 + \sqrt{a_2 p_s}x_2) + n_{D_2} \tag{3.14}$$

where n_{D_1} and n_{D_2} denote AWGN with zero mean and variance σ^2 , h_{SD_1} and h_{SD_2} are the fading channel coefficients, a_i *is* power coefficient for symbol x_i, i=1,2, and p_s is transmission power at the S. As user1 is far away from the base station compared to user2 so, $a_1 \geq a_2$. The received SINR at D_1 to detect its symbol x_1 is given by

$$\gamma_1 = \frac{a_1 \rho_s |h_{SD_1}|^2}{a_2 \rho_s |h_{SD_1}|^2 + 1} \tag{3.15}$$

The received SINR at D_2 to detect symbol x_1 is given by

$$\gamma_{1,2} = \frac{a_1 \rho_s |h_{SD_2}|^2}{a_2 \rho_s |h_{SD_2}|^2 + 1} \tag{3.16}$$

The received SINR at D_2 to detect its symbol x_2 after SIC is given by

$$\gamma_2 = a_1 \rho_s |h_{SD_2}|^2 \tag{3.17}$$

Energy Harvesting Phase: The received signal at selected relay k^* from S during sub-block time αT is

$$y_{R_{k^*}} = h_{SR_{k^*}}(\sqrt{a_1 p_s}x_1 + \sqrt{a_2 p_s}x_2) + n_{R_{k^*}} \tag{3.18}$$

where $n_{R_{k^*}}$ represents AWGN at relay k^* having zero mean and variance σ^2. The harvested energy is as follows:

$$E_H = |h_{SR_{k^*}}|^2 p_s \alpha T \eta \tag{3.19}$$

where, η is energy harvesting efficiency.

The transmission power at R_{k^*} for forwarding the decoded signal to both users is

$$P_T = \frac{E_H}{(1-\alpha)T/2} \tag{3.20}$$

Decoding Phase: The received signal at selected relay k^* from S during sub-block time $(1-\alpha)\frac{T}{2}$ is

$$y_{R_{k^*}} = h_{R_{k^*}}(\sqrt{a_1 p_s}x_1 + \sqrt{a_2 p_s}x_2) + n_{R_{k^*}} \tag{3.21}$$

The received SINR at R_{k^*} to symbol x_1 is given by

$$\gamma_{R,1} = \frac{a_1 \rho_s |h_{SR_{k^*}}|^2}{a_2 \rho_s |h_{SR_{k^*}}|^2 + 1} \tag{3.22}$$

The received SINR at R_{k^*} to detect symbol x_2 after SIC is given by

$$\gamma_{R,2} = a_2 \rho_s |h_{SR_{k^*}}|^2 \tag{3.23}$$

With the harvested energy, the relay R_{k^*} will forward the decoded signal to both users in the second phase

Second Phase: The received signal at D_1 and D_2 in the second phase can be expressed as

$$y_1^{DF} = h_{R_{k^*}D_1}\left(\sqrt{a_1 P_T} x_1 + \sqrt{a_2 P_T} x_2\right) + n_1 \tag{3.24}$$

$$y_2^{DF} = h_{R_{k^*}D_2}\left(\sqrt{a_1 P_T} x_1 + \sqrt{a_2 P_T} x_2\right) + n_2 \tag{3.25}$$

where n_1 and n_2 represent the AWGN at D_1 and D_2 , respectively, with zero mean and variance σ^2 and transmission power at relay is P_T.

The received SINR at D_1 to detect its symbol x_1 is given by

$$\gamma_1^{DF} = \frac{a_1 \phi_E \rho_s |h_{SR_{k^*}}|^2 |h_{R_{k^*}D_1}|^2}{a_2 \phi_E \rho_s |h_{SR_{k^*}}|^2 |h_{R_{k^*}D_1}|^2 + 1} \tag{3.26}$$

$$\text{where,} \;\; \phi_E = \frac{2\alpha\eta}{1-\alpha} \tag{3.27}$$

The received SINR at D_2 to detect symbol x_1 is given by

$$\gamma_{1,2}^{DF} = \frac{a_1 \phi_E \rho_s |h_{SR_{k^*}}|^2 |h_{R_{k^*}D_2}|^2}{a_2 \phi_E \rho_s |h_{SR_{k^*}}|^2 |h_{R_{k^*}D_2}|^2 + 1} \tag{3.28}$$

The received SINR at D_2 to detect its symbol x_2 after SIC is given by

$$\gamma_2^{DF} = a_2 \phi_E \rho_s |h_{SR_{k^*}}|^2 |h_{R_{k^*}D_2}|^2 \tag{3.29}$$

3.4 Performance Analysis

3.4.1 Outage Probability Analysis of user1

The outage probability of the D_1 is given by

$$P_1 = P\left(\max\left(\gamma_{SD_1}, \gamma_{R_{k^*}D_1}\right) < \gamma_{th}\right) \tag{3.30}$$

where γ_{th} is SINR threshold

$$P_1 = P\left(\gamma_{SD_1} < \gamma_{th} \cap \gamma_{R_{k^*}D_1} < \gamma_{th}\right) \tag{3.31}$$

$$P_1 = P\left(\gamma_{SD_1} < \gamma_{th}\right) P\left(\gamma_{R_{k^*}D_1} < \gamma_{th}\right) \tag{3.32}$$

After simplifying the above equation, we can rewrite it as follows

$$P_1 = P\left(\gamma_1 < \gamma_{th}\right)\left(1 - P\left(\gamma_{R,1} > \gamma_{th} \cap \gamma_{R,2} > \gamma_{th} \cap \gamma_1^{DF} > \gamma_{th}\right)\right) \tag{3.33}$$

After simplifying the above equation, we can rewrite it as follows

$$P_1 = P\left(\gamma_1 < \gamma_{th}\right) P\left(\gamma_{R,1} < \gamma_{th} \cup \gamma_{R,2} < \gamma_{th} \cup \gamma_1^{DF} < \gamma_{th}\right) \tag{3.34}$$

After, substituting (3.15), (3.22), (3.23), (3.26) in (3.34), we get

$$P_1 = P\left(|h_{SD_1}|^2 < \tau\right)\left(1 - P\left(|h_{SR_{k^*}}|^2 > \theta \cap \frac{a_1\phi_E\rho_s|h_{SR_{k^*}}|^2|h_{R_{k^*}D_1}|^2}{a_2\phi_E\rho_s|h_{SR_{k^*}}|^2|h_{R_{k^*}D_1}|^2+1} > \gamma_{th}\right)\right) \tag{3.35}$$

$$\text{where,}\quad \tau = \frac{\gamma_{th}}{(a_1 - a_2\gamma_{th})\,\rho_s},\ v = \frac{\gamma_{th}}{a_2\rho_s},\ \theta = \max(\tau, v); \tag{3.36}$$

After, substituting (3.1), (3.12), (3.3) in (3.35), we get

$$\begin{aligned} P_1 = \left[1 - \exp\left(\frac{-\tau}{\Omega_{SD_1}}\right)\right]\Bigg[1 - \sum_{k=1}^{k=K}\binom{K}{k}(-1)^{(k-1)}\left(\frac{k}{\Omega_{SR_{k^*}}}\right) \\ \times \int_{\theta}^{\infty}\exp\left(\frac{-\tau'}{x\Omega_{R_{k^*}D_1}}\right)\exp\left(\frac{-xk}{\Omega_{SR_{k^*}}}\right)dx\Bigg] \end{aligned} \tag{3.37}$$

$$\text{where,}\quad \tau = \frac{\gamma_{th}}{(a_1 - a_2\gamma_{th})\,\phi_E\rho_s} \tag{3.38}$$

The integral $\int_{\theta}^{\infty}\exp\left(\frac{-\tau'}{x\Omega_{R_{k^*}D_1}}\right)\exp\left(\frac{-xk}{\Omega_{SR_{k^*}}}\right)dx$ can be solved by using Chebyshev gauss quadrature and by 1^{st} order modified Bessel function of the second kind [8, Eq. (3.324.1)].

By using Chebyshev gauss quadrature and first-order modified Bessel function of the second kind, the above equation can be rewritten as follows

$$\begin{aligned} P_1 \approx \left[1 - \exp\left(\frac{-\tau}{\Omega_{SD_1}}\right)\right]\Bigg[1 - \sum_{k=1}^{k=K}\binom{K}{k}(-1)^{(k-1)}\left(\frac{k}{\Omega_{SR_{k^*}}}\right) \\ \times\Bigg[2\sqrt{\frac{\tau'\Omega_{SR_{k^*}}}{k\Omega_{R_{k^*}D_1}}}K_1\left(2\sqrt{\frac{\tau' k}{\Omega_{SR_{k^*}}\Omega_{R_{k^*}D_1}}}\right) - \sum_{i=1}^{S}W_i\sqrt{1-t_{i2}} \\ \times\exp\left(\frac{-\tau'2}{(t_i+1)\,\theta\Omega_{R_{k^*}D_1}}\right)\exp\left(\frac{-(t_i+1)\,\theta k}{2\Omega_{SR_{k^*}}}\right)\Bigg]\Bigg] \end{aligned} \tag{3.39}$$

where, $K_1(.)$ represents the first-order modified Bessel function of the second kind. [**gradshteyn2007**], $W_i = \pi/S$, $t_i = \cos\left(\frac{2i-1}{2S}\pi\right)$

3.4.2 Outage Probability Analysis of user2

The outage probability of the D_2 is given by

$$P_2 = P\left(\max\left(\gamma_{SD_2}, \gamma_{R_{k^*}D_2}\right) < \gamma_{th}\right) \tag{3.40}$$

$$= P\left(\gamma_{SD_2} < \gamma_{th} \cap \gamma_{R_{k^*}D_2} < \gamma_{th}\right) \tag{3.41}$$

$$= P\left(\gamma_{SD_2} < \gamma_{th}\right)P\left(\gamma_{R_{k^*}D_2} < \gamma_{th}\right) \tag{3.42}$$

After simplifying the above equation, we can rewrite it as follows

$$P_2 = P\left(\gamma_{1,2} < \gamma_{th} \cup \gamma_2 < \gamma_{th}\right)P\left(\gamma_{R,1} < \gamma_{th} \cup \gamma_{R,2} < \gamma_{th} \cup \gamma_{1,2}^{DF} < \gamma_{th} \cup \gamma_2^{DF} < \gamma_{th}\right) \tag{3.43}$$

After simplifying the above equation, we can rewrite it as follows

$$P_2 = \left(1 - P\left(\gamma_{1,2} > \gamma_{th} \cap \gamma_2 > \gamma_{th}\right)\right)\left(1 - P\left(\gamma_{R,1} > \gamma_{th} \cap \gamma_{R,2} > \gamma_{th} \cap \gamma_{1,2}^{DF} > \gamma_{th} \cap \gamma_2^{DF} > \gamma_{th}\right)\right) \quad (3.44)$$

After substituting (3.16), (3.17) (3.22), (3.23), (3.28), (3.29) in (3.44), we get

$$P_2 = \left[1 - P\left(|h_{SD_2}|^2 > \theta\right)\right]\left[1 - P\left(|h_{SR_{k^*}}|^2 > \theta \cap |h_{SR_{k^*}}|^2 |h_{R_{k^*}D_2}|^2 > \theta^{'}\right)\right] \quad (3.45)$$

$$\text{where, } \tau^{'} = \frac{\gamma_{th}}{(a_1 - a_2\gamma_{th})\,\rho_s\phi_E},\ v^{'} = \frac{\gamma_{th}}{a_2\rho_s\phi_E},\ \theta^{'} = \max\left(\tau^{'}, v^{'}\right) \quad (3.46)$$

After substituting (3.1), (3.12), (3.3) in (3.45), we get

$$P_2 = \left[1 - \exp\left(\frac{-\theta}{\Omega_{SD_2}}\right)\right]\left[1 - \sum_{k=1}^{k=K}\binom{K}{k}(-1)^{(k-1)}\left(\frac{k}{\Omega_{SR_{k^*}}}\right) \times \int_{\theta}^{\infty}\exp\left(\frac{-\theta^{'}}{x\Omega_{R_{k^*}D_2}}\right)\exp\left(\frac{-xk}{\Omega_{SR_{k^*}}}\right)dx\right] \quad (3.47)$$

The integral $\int_{\theta}^{\infty}\exp\left(\frac{-\theta^{'}}{x\Omega_{R_{k^*}D_2}}\right)\exp\left(\frac{-xk}{\Omega_{SR_{k^*}}}\right)dx$ can be solved by using Chebyshev gauss quadrature and by 1st order modified Bessel function of the second kind [8, Eq. (3.324.1)].

By using Chebyshev gauss quadrature and first-order modified Bessel function of the second kind, the above equation can be rewritten as follows

$$P_2 \approx \left[1 - \exp\left(\frac{-\theta}{\Omega_{SD_2}}\right)\right]\left[1 - \sum_{k=1}^{k=K}\binom{K}{k}(-1)^{(k-1)}\left(\frac{k}{\Omega_{SR_{k^*}}}\right) \times \left[2\sqrt{\frac{\theta^{'}\Omega_{SR_{k^*}}}{k\Omega_{R_{k^*}D_2}}}K_1\left(2\sqrt{\frac{\theta^{'}k}{\Omega_{SR_{k^*}}\Omega_{R_{k^*}D_2}}}\right) - \sum_{i=1}^{S}W_i\sqrt{1-t_{i^2}} \times \exp\left(\frac{-\theta^{'}2}{(t_i+1)\,\theta\Omega_{R_{k^*}D_2}}\right)\exp\left(\frac{-(t_i+1)\,\theta k}{2\Omega_{SR_{k^*}}}\right)\right]\right] \quad (3.48)$$

Asymptotic outage probability of D_1:

Using McLaurin's expression, we have $e^x = 1 + x$ for small value of x. So by using (3.39), the asymptotic outage probability of D_1 is obtained as follows:

$$P_{1,\infty} \approx \left[\frac{\tau}{\Omega_{SD_1}}\right]\left[1 - \sum_{k=1}^{k=K}\binom{K}{k}(-1)^{(k-1)}\left(\frac{k}{\Omega_{SR_{k^*}}}\right) \times \int_{\theta}^{\infty}\left(1 - \frac{-\tau^{'}}{x\Omega_{R_{k^*}D_1}}\right)\exp\left(\frac{-xk}{\Omega_{SR_{k^*}}}\right)dx\right] \quad (3.49)$$

By using [8, Eq. (3.352.4)], the above equation can be rewritten as follows

$$P_{1,\infty} \approx \left[\frac{\tau}{\Omega_{SD_1}}\right]\left[1 - \sum_{k=1}^{k=K}\binom{K}{k}(-1)^{(k-1)}\left(\frac{k}{\Omega_{SR_{k^*}}}\right)\left[\frac{\Omega_{SR_{k^*}}}{k}\exp\left(\frac{-\theta k}{\Omega_{SR_{k^*}}}\right) + \frac{\tau^{'}}{\Omega_{R_{k^*}D_1}}Ei\left(\frac{-k\theta}{\Omega_{SR_{k^*}}}\right)\right]\right] \quad (3.50)$$

where, $Ei(-x) \approx E_c + ln(x)$ for small value of x, E_c is euler's constant, and $E_c = -\lim_{s\to\infty}\left(\sum_{m=1}^{m=} \frac{1}{m} - ln(s)\right)$

Asymptotic outage probability of D_2:

Using McLaurin's expression, we have $e^x = 1 + x$ for small value of x. So by using the asymptotic outage probability of D_2 is given as follows:

$$P_{2,\infty} \approx \left[\frac{-\theta}{\Omega_{SD_2}}\right]\left[1 - \sum_{k=1}^{k=K}\binom{K}{k}(-1)^{(k-1)}\left(\frac{k}{\Omega_{SR_{k^*}}}\right)\left[\frac{\Omega_{SR_{k^*}}}{k}\exp\left(\frac{-\theta k}{\Omega_{SR_{k^*}}}\right) + \frac{\theta'}{\Omega_{R_{k^*}D_1}} Ei\left(\frac{-k\theta}{\Omega_{SR_{k^*}}}\right)\right]\right] \tag{3.51}$$

Diversity order of both users: The diversity order of user1 is

$$d_1 = -\lim_{\rho\to\infty}\frac{\log(P_1(\rho_s))}{\log(\rho)} \tag{3.52}$$

After substituting (3.50) in (3.52), d_1 is obtained as 2

The diversity order of user2 is

$$d_2 = -\lim_{\rho\to\infty}\frac{\log(P_2(\rho_s))}{\log(\rho)} \tag{3.53}$$

After, substituting (3.51) in (3.53), d_2 is obtained as 2

3.4.3 Ergodic Capacity Analysis of user1

The ergodic capacity of the user1 is given by

$$C_1 = E\left[\frac{1}{2}log_2(1+Z_1)\right] \tag{3.54}$$

where W_1 is a random variable and W_1 = max $\left(\gamma_1, \min\left(\gamma_{R,1}, \gamma_1^{DF}\right)\right)$

$$C_1 = \frac{1}{2\ln(2)}\int_0^\infty \frac{1 - F_{Z_1}(x)}{1+x}dx \tag{3.55}$$

$$\text{where } F_{Z_1}(x) = P\left(\max\left(\gamma_1, \min\left(\gamma_{R,1}, \gamma_1^{DF}\right)\right)\right) \tag{3.56}$$

$$F_{Z_1}(x) = P\left(\gamma_1 < x \cap \min\left(\gamma_{R,1}, \gamma_1^{DF}\right) < x\right) \tag{3.57}$$

After simplifying the above equation, we can rewrite it as follows

$$F_{Z_1}(x) = P(\gamma_1 < x)\left(1 - P\left(\max\left(\gamma_{R,1}, \gamma_1^{DF}\right) > x\right)\right) \tag{3.58}$$

After, substituting (3.1), (3.12), (3.3) in (3.58), we get

$$F_{Z_1}(x) = P\left(|h_{SD_1}|^2 < \mu\right)\left(1 - P\left(|h_{SR_{k^*}}|^2 > \mu \cap |h_{SR_{k^*}}|^2|h_{R_{k^*}D_1}|^2 > \frac{\mu}{\phi_E}\right)\right) \tag{3.59}$$

$$\text{where } \mu = \frac{x}{(a_1 - a_2 x)\rho_s} \tag{3.60}$$

After substituting (3.1), (3.22), (3.26) in (3.59), we get

$$F_{Z_1}(x) = \left[1 - \exp\left(\frac{-\mu}{\Omega_{SD_1}}\right)\right]\left[1 - \sum_{k=1}^{k=K}\binom{K}{k}(-1)^{(k-1)}\left(\frac{k}{\Omega_{SR_{k^*}}}\right)\right.$$
$$\left.\times\int_{\mu}^{\infty}\exp\left(\frac{-\mu}{y\phi_E\Omega_{R_{k^*}D_1}}\right)\exp\left(\frac{-yk}{\Omega_{SR_{k^*}}}\right)dy\right] \tag{3.61}$$

The above equation is valid if $x < \frac{a_1}{a_2}$

After, substituting (3.61) in (3.55), we get

$$C_1 = \frac{1}{2\ln(2)}\int_0^{\frac{a_1}{a_2}}\frac{\mathscr{C}}{1+x}dx \tag{3.62}$$

$$\text{where}\quad \mathscr{C} = \exp\left(\frac{-\mu}{\Omega_{SD_1}}\right) + \left[1 - \exp\left(\frac{-\mu}{\Omega_{SD_1}}\right)\right]\left[\sum_{k=1}^{k=K}\binom{K}{k}(-1)^{(k-1)}\left(\frac{k}{\Omega_{SR_{k^*}}}\right)\right.$$
$$\left.\int_{\mu}^{\infty}\exp\left(\frac{-\mu}{y\phi_E\Omega_{R_{k^*}D_1}}\right)\exp\left(\frac{-yk}{\Omega_{SR_{k^*}}}\right)dy\right] \tag{3.63}$$

3.4.4 Ergodic Capacity Analysis of user2

The ergodic capacity of the user2 is given by

$$C_2 = E\left[\frac{1}{2}log_2(1+Z_2)\right] \tag{3.64}$$

where Z_2 is a random variable and Z_2 = max $\left(\gamma_2, \min\left(\gamma_{R,2}, \gamma_2^{DF}\right)\right)$

$$C_2 = \frac{1}{2\ln(2)}\int_0^{\infty}\frac{1 - F_{Z_2}(x)}{1+x}dx \tag{3.65}$$

$$\text{where } F_{Z_2}(x) = P\left(\max\left(\gamma_2, \min\left(\gamma_{R,2}, \gamma_2^{DF}\right)\right)\right) \tag{3.66}$$

$$F_{Z_2}(x) = P\left(\gamma_2 < x \cap \min\left(\gamma_{R,2}, \gamma_2^{DF}\right) < x\right) \tag{3.67}$$

After simplifying the above equation, we can rewrite it as follows

$$F_{Z_2}(x) = P(\gamma_2 < x)\left(1 - P\left(\max\left(\gamma_{R,2}, \gamma_2^{DF}\right) > x\right)\right) \tag{3.68}$$

After, substituting (3.17), (3.23), (3.29) in (3.68), we get

$$F_{Z_2}(x) = P\left(|h_{SD_2}|^2 < \frac{x}{a_2\rho_s}\right)\left(1 - P\left(|h_{SR_{k^*}}|^2 > \frac{x}{a_2\rho_s} \cap |h_{SR_{k^*}}|^2|h_{R_{k^*}D_1}|^2 > \frac{x}{a_2\rho_s\phi_E}\right)\right) \tag{3.69}$$

After, substituting (3.1), (3.12), (3.3) in (3.69), we get

$$F_{Z_2}(x) = \left[1 - \exp\left(\frac{-x}{a_2\rho_s\Omega_{SD_2}}\right)\right]\left[1 - \sum_{k=1}^{k=K}\binom{K}{k}(-1)^{(k-1)}\left(\frac{k}{\Omega_{SR_{k^*}}}\right)\right.$$
$$\left.\times\int_{\frac{x}{a_2\rho_s}}^{\infty}\exp\left(\frac{-x}{ya_2\phi_E\rho_s\Omega_{R_{k^*}D_2}}\right)\exp\left(\frac{-yk}{\Omega_{SR_{k^*}}}\right)dy\right] \tag{3.70}$$

After, substituting (3.70) in (3.65), we can rewrite it as follows

$$C_2 = \frac{1}{2\ln(2)} \int_0^{\infty} \frac{\mathscr{D}}{1+x} dx \tag{3.71}$$

$$\begin{aligned} where \quad \mathscr{D} = \exp\left(\frac{-x}{a_2\rho_s\Omega_{SD_2}}\right) + \left[1 - \exp\left(\frac{-x}{a_2\rho_s\Omega_{SD_2}}\right)\right]\Bigg[\sum_{k=1}^{k=K}\binom{K}{k}(-1)^{(k-1)}\left(\frac{k}{\Omega_{SR_{k^*}}}\right) \\ \int_{\frac{x}{a_2\rho_s}}^{\infty} \exp\left(\frac{-x}{ya_2\phi_E\rho_s\Omega_{R_{k^*}D_2}}\right)\exp\left(\frac{-yk}{\Omega_{SR_{k^*}}}\right)dy\Bigg] \end{aligned} \tag{3.72}$$

3.4.5 Overall System Throughput

The overall system throughput is given by

$$R = (1-P_1)R_1 + (1-P_2)R_2 \tag{3.73}$$

where P_1 and P_2 are obtained from (3.39) and (3.51) respectively. R_1 and R_2 are target rates of user1 and user2 respectively.

3.5 Energy Efficiency

Energy efficiency is a ratio of total data rate and total energy consumption. Where total data rate is overall system throughput. So, the expression for energy efficiency is as follows

$$\eta = \frac{2R}{T\,(p_s + P_T)} \tag{3.74}$$

After substituting p_s and P_T, the above equation can be rewritten as follows

$$\eta = \frac{2R}{\rho_s\left(1 + \psi_E\Omega_{SR_{k^*}}\right)} \tag{3.75}$$

3.6 Numerical Results and Discussions

In this section, we will analyze the derived closed-form expressions. We also demonstrate the effects of various parameters on outage probability, overall system throughput, ergodic capacity for the proposed system model. For numerical investigation, we set $a_1 = 0.7$, $a_2 = 0.3$, γ_{th} = 2 dB, $n_p = 4$, $R_1 = 1.5, R_2 = 1.5$, $\Omega_{SD_1} = (1)^{-4}$, $\Omega_{SD_2} = (0.75)^{-4}$, $\Omega_{SR_{k^*}} = (0.5)^{-4}$, $\Omega_{R_{k^*}D_1} = (0.5)^{-4}$, and $\Omega_{R_{k^*}D_2} = (0.25)^{-4}$, =0.7, $\eta = 0.8$, S = 4.

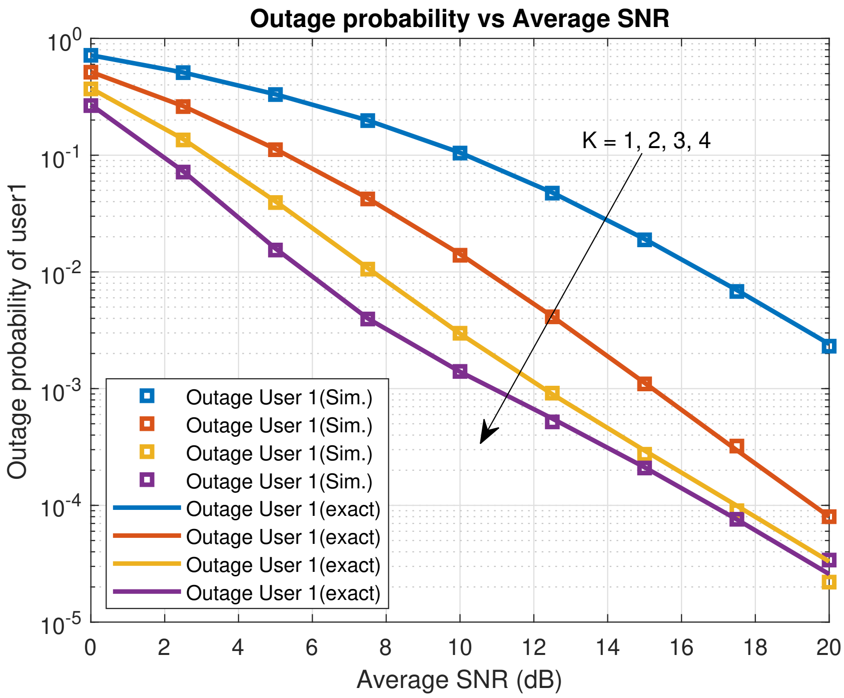

Figure 3.2: Outage probability vs. average SNR of user1 for different values of K

Figure 3.2 shows the effect of K on the outage probability of the user2. From the plot, we can observe that with the increase in value of K, the outage performance improves because if more relays are employed in this system, then the best relay can be selected out of K relays. To achieve the outage probability of 10^{-2}, the SNR required for the system with K=1, K=2, K=3, and K=4 are 16.5 dB, 10.5 dB, 7.5 dB, 6 dB, respectively. So the SNR gain achieved by the system with K=2, K=3, K=4 w.r.t system with K=1 are 6 dB, 9 dB, 10.5 respectively. So, it has been inferred that with the increase in value of K above 3, there is no improvement in SNR gain. When SNR increases, the outage probability tends to decrease. It is because as SNR increases, the signal becomes much stronger than the noise.

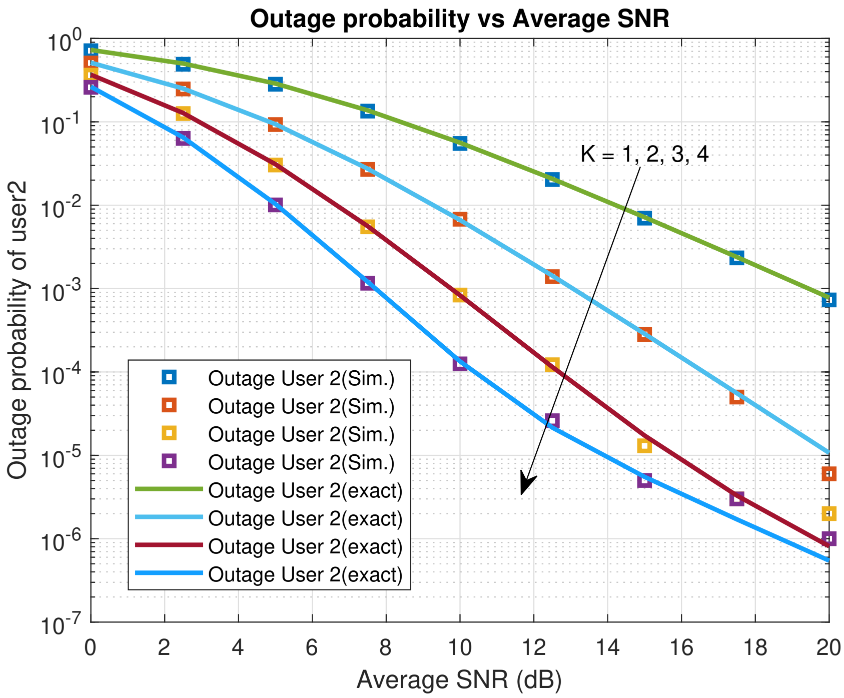

Figure 3.3: Outage Probability vs. Average SNR of user2 for different values of K

Figure 3.3 shows the effect of value of K on the outage probability of the user2. From the plot, we can observe that with the increase in the number of relays, the outage performance improves because if more relays are employed in this system model, then the best relay can be selected out of K relays. To achieve the outage probability of 10^{-2}, the SNR required for the system with K=1, K=2, K=3, and K=4 are 14 dB, 9.5 dB, 6.5 dB, 5 dB, respectively. So, the SNR gain achieved by the system with K=2, K=3, and K=4 w.r.t system with K=1 are 4.5 dB, 7.5 dB, 9 dB respectively. So, it has been inferred that with the increase in value of K above 3, there is not much improvement in SNR gain.

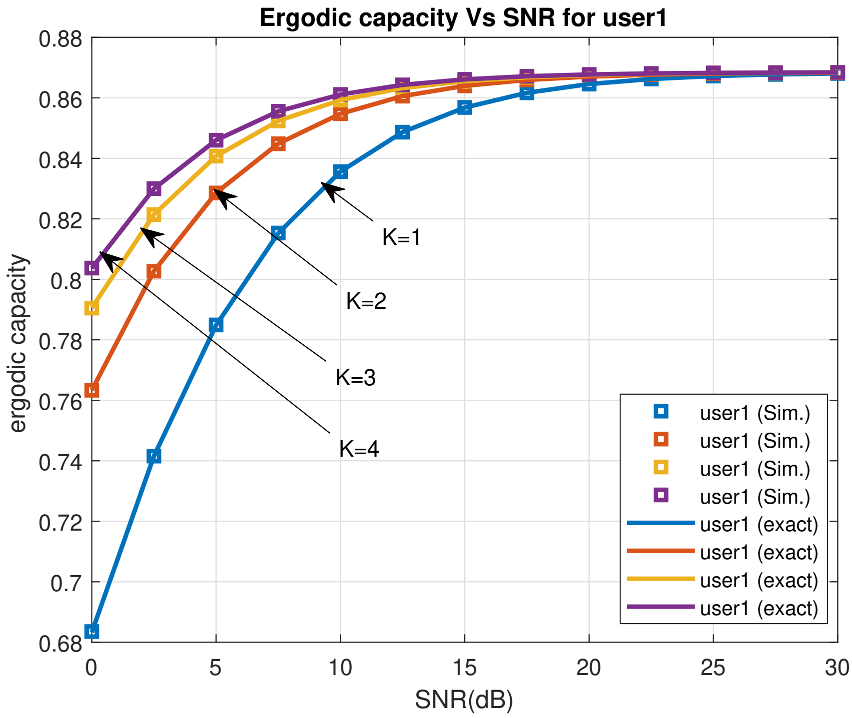

Figure 3.4: Ergodic Capacity vs. Average SNR of user1 for different values of K

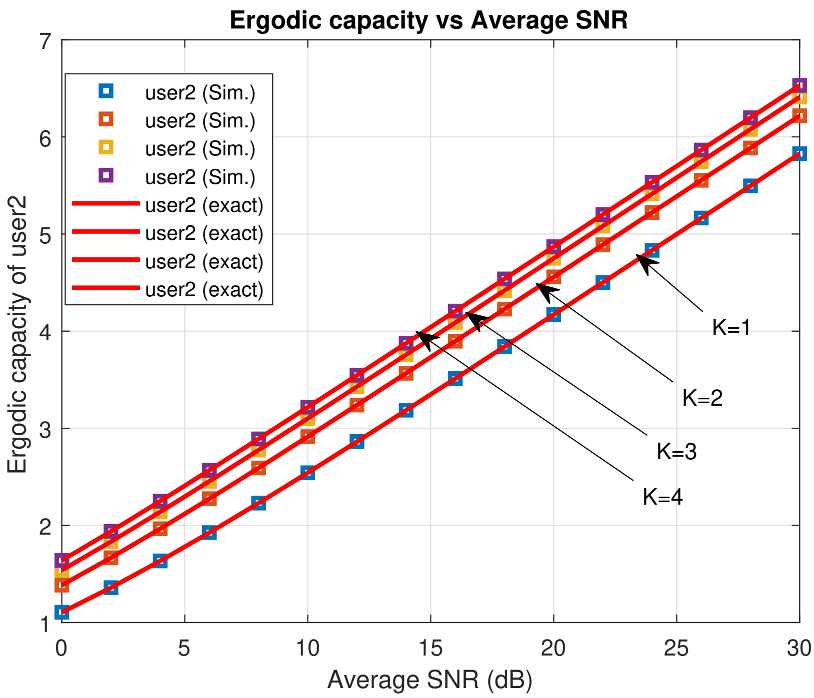

Figure 3.5: Ergodic Capacity vs. Average SNR of user2 for different values of K

Figure 3.4 and 3.5 shows the effect of the number of relays on the ergodic capacity of the user1 and user2 respectively. From both figures, we can observe that with the increase in value of K, the ergodic capacity increases slightly. For user1, the ergodic capacity saturates at high SNR. It is because user1 decodes its signal by considering the user2 signal as noise. For user2, the ergodic capacity increases linearly with SNR. It is because while decoding its signal, the user2 has no interference with the user1 signal.

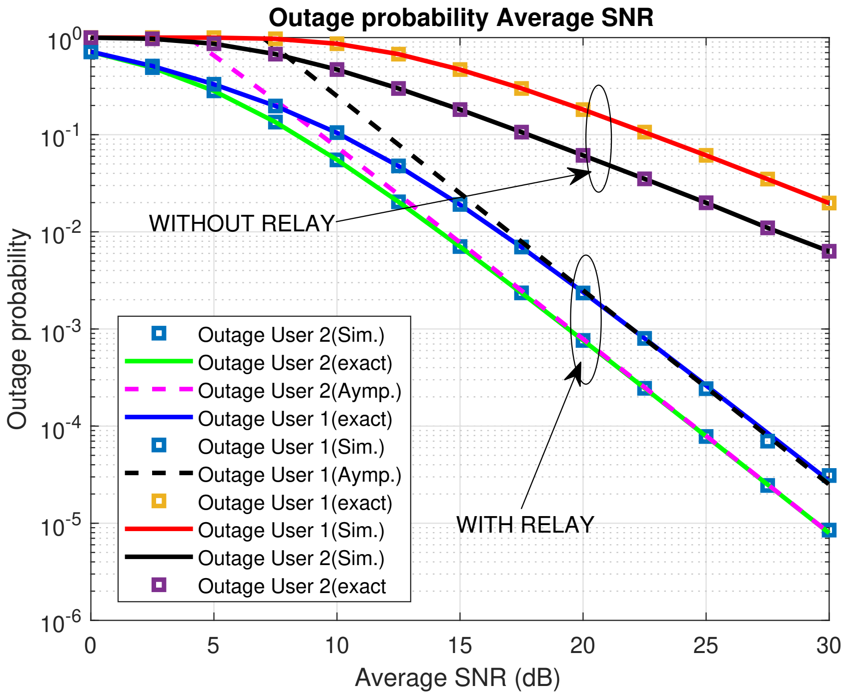

Figure 3.6: Outage Probability vs. Average SNR for system with relay and system without relay

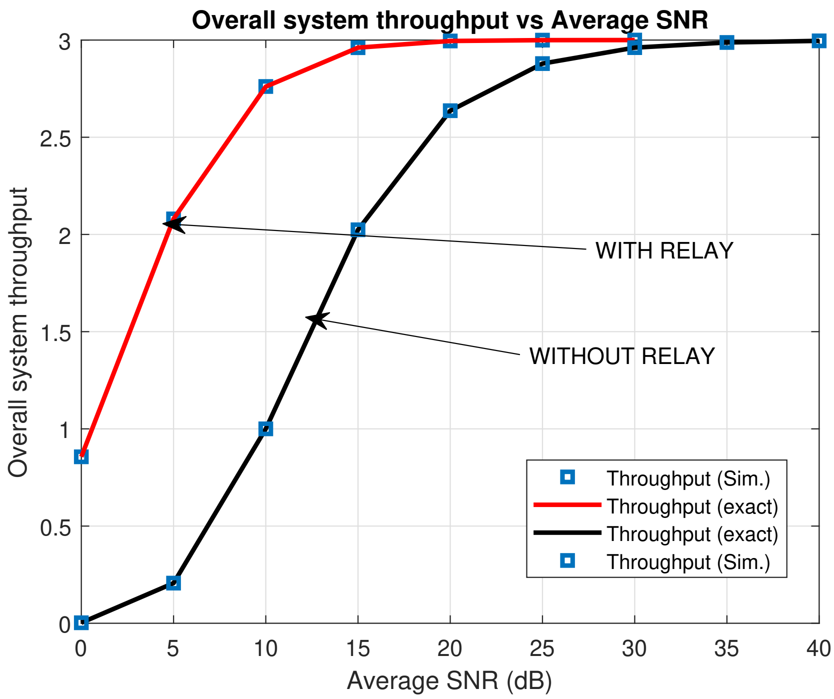

Figure 3.7: Throughput vs. Average SNR for system with relay and system without relay

Figure 3.6 and 3.7 shows the impact of the relay on the outage probability and overall system throughput respectively. From both plots, we can observe that system with a relay has better performance than system without a relay in terms of both outage probability and throughput. It has been inferred from figure 2.6 that to obtain the outage probability of 10^{-2}, SNR required for the system with a relay is 13 dB lesser when compared to the system without a relay, and from Figure (2.7) that to obtain throughput of 2.5 bits/sec/Hz, SNR required for the system with a relay is 10 dB lesser when compared to the system without a relay. When SNR increases, the throughput tends to increase and saturates at high SNR. It is because, at high SNR, outage probability is almost zero. So throughput will be the sum of target rates of both users.

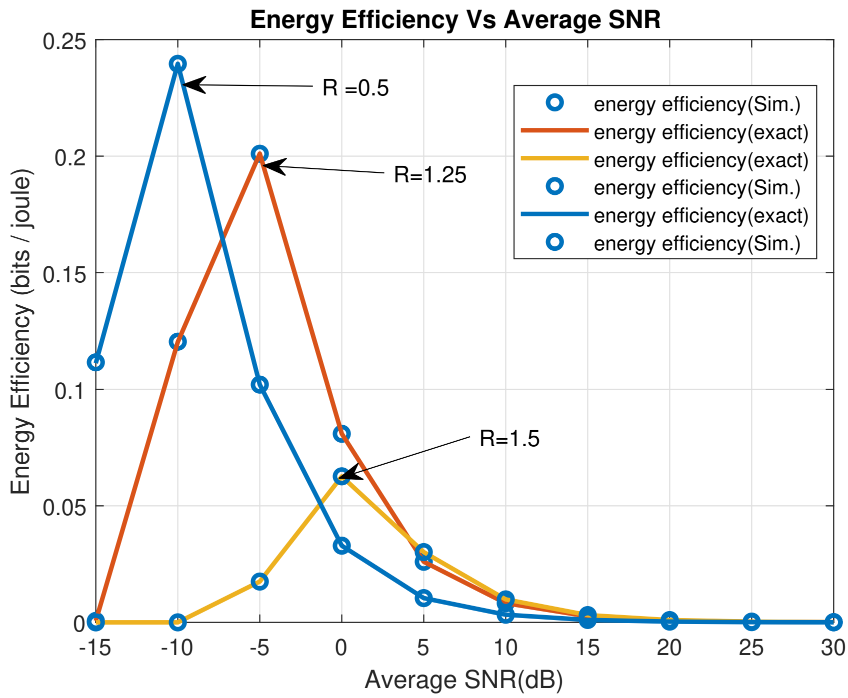

Figure 3.8: Energy Efficiency vs. Average SNR

Figure 3.8 shows the effect of the target rate on the energy efficiency. From the figure, one can observe that the system attains maximum energy efficiency at a particular SNR value, and also when the target rate changes, the peak of the energy efficiency is also varying. Energy efficiency is higher at lower SNR regions and lower at higher SNR regions. This is because, at higher SNR regions, power consumed by the system is more than the achieved overall system throughput.

3.7 Conclusions

In this chapter, the performance analysis of the SWIPT-enabled cooperative NOMA system model for DF networks is carried out by deriving the outage probability, ergodic capacity expressions, energy efficiency, and overall system throughput expressions in closed-from over Rayleigh fading channels.

Furthermore, closed-form expressions for performance metrics such as outage probability, ergodic capacity, energy efficiency, and overall system throughput of the proposed system model are implemented in MATLAB. From simulation results, it is observed that the outage performance of the proposed system model for both users improves with the increase in value of K, outage performance for the system with relay is better than the system without relay, and also, there is improvement in diversity gain of the system with relays. Also, it is observed that ergodic capacity for user1 saturates at high SNR, while ergodic capacity for user2 proportionally increases with SNR. It is inferred from the simulation results that the ergodic capacity of both users increases with an increase in value of K. From high SNR analysis of outage probability, the diversity order of 2 is obtained. Further, when the target rate changes, the peak of energy efficiency also varies. Finally, the simulated outage probability, ergodic capacity, energy efficiency, and overall system throughput values obtained from Monte Carlo simulations agree well with the theoretical outage probability and ergodic capacity values. Therefore, the derived expressions are validated using simulations as well.

Chapter 4

SWIPT Enabled Cooperative NOMA Networks for 5G and Beyond Wireless Communication Systems with Imperfect CSI and SIC

4.1 Introduction

The exact expressions for performance metrics of the SWIPT-enabled cooperative NOMA system model for DF networks are derived over Rayleigh fading channels in chapter 3. The proposed system model in chapter 3 has achieved reliability, spectral efficiency, and energy efficiency. In chapter 3, performance analysis is carried out by assuming perfect CSI and perfect SIC. However, practically perfect CSI and perfect SIC are not possible at receiver or transmitter nodes. Thus, to make our system applicable to the practical scenario, we must consider imperfect CSI and imperfect SIC. Chapter 4 is an extended version of the chapter 3 system model, where imperfect CSI and imperfect SIC are considered at all nodes. In this chapter, we discuss the SWIPT-enabled cooperative NOMA system model for DF networks with imperfect CSI and imperfect SIC. The performance of this proposed system is analyzed by deriving the exact outage probability and ergodic capacity expressions over Rayleigh fading channels.

4.2 Organisation of Chapter

The rest of the chapter is organized as follows: The system model for a SWIPT-enabled cooperative NOMA system for DF networks with imperfect CSI and imperfect SIC has been discussed in Section 4.3. Section 4.4 provides the closed-form expressions for outage probability and ergodic capacity of both mobile users over Rayleigh fading channels. Furthermore, Numerical results and inferences are given in Section 4.5. Finally, the concluding remarks are given in Section 4.6.

4.3 System Model

In this chapter, we have considered the imperfect CSI. So the estimate for the channel $h_{i,j}$ is $\hat{h}_{i,j}$, which is defined as follows:

$$h_{i,j} = \hat{h}_{i,j} + e_{i,j} \tag{4.1}$$

where $e_{i,j}$ stands for channel estimation error which follows the complex Gaussian distribution with zero mean and variance $\sigma^2_{i,j}$. The channel estimate $\hat{h}_{i,j}$ also follows the complex Gaussian distribution with zero mean and variance $\hat{\Omega}_{i,j} = d_{i,j}^{-n_p} - \sigma^2_{i,j}$. The CDF of random variables $|\hat{h}_{SD_i}|^2$, $|\hat{h}_{SR_k}|^2$, $|\hat{h}_{R_kD_i}|^2$ are given by

$$F_{|\hat{h}_{SD_i}|^2}(x) = 1 - \exp\left(\frac{-x}{\hat{\Omega}_{SD_i}}\right) \tag{4.2}$$

$$F_{|\hat{h}_{SR_k}|^2}(y) = 1 - \exp\left(\frac{-y}{\hat{\Omega}_{SR_k}}\right) \tag{4.3}$$

$$F_{|\hat{h}_{R_kD_i}|^2}(z) = 1 - \exp\left(\frac{-z}{\hat{\Omega}_{R_kD_i}}\right) \tag{4.4}$$

Out of multiple relays, one relay is selected and that chosen relay will harvest energy from S, decode the signal received from S and then forward the decoded signal to both users with the harvested energy the forwarding phase.

The PRS strategy is employed to select relay based on the instantaneous SNR between S$\rightarrow$ R_k. Let the selected relay index is k^* and its respective instantaneous SNR is given as follows:

$$k^* = arg \max_{k=1,....K} \ \rho_s|\hat{h}_{SR_k}|^2 \tag{4.5}$$

$$\rho_s|\hat{h}_{SR_{k^*}}|^2 = \max_{k=1,....K} \ \rho_s|\hat{h}_{SR_k}|^2 \tag{4.6}$$

The CDF of the selected relay k^* is

$$F_{|\hat{h}_{SR_{k^*}}|^2}(x) = P\left(|\hat{h}_{SR_{k^*}}|^2 < x\right) \tag{4.7}$$

$$F_{|\hat{h}_{SR_{k^*}}|^2}(x) = P\left(\max\left(|\hat{h}_{SR_1}|^2, |\hat{h}_{SR_2}|^2, ...|\hat{h}_{SR_k}|^2\right) < x\right) \tag{4.8}$$

After simplifying the above equation, we can rewrite it as follows

$$F_{|\hat{h}_{SR_{k^*}}|^2}(x) = \prod_{k=1}^{K} P\left(|\hat{h}_{SR_k}|^2 < x\right) \tag{4.9}$$

After substituting (4.3) in (:9), the CDF of selected relay is as follows:

$$F_{|\hat{h}_{SR_{k^*}}|^2}(x) = \prod_{k=1}^{K}\left[1 - \exp\left(\frac{-x}{\hat{\Omega}_{SR_k}}\right)\right] \tag{4.10}$$

Let $\hat{\Omega}_{SR_1} = \hat{\Omega}_{SR_2} = ...\hat{\Omega}_{SR_K}$

Now CDF of the selected relay k^* is

$$F_{|\hat{h}_{SR_{k^*}}|^2}(x) = \left[1 - \exp\left(\frac{-x}{\hat{\Omega}_{SR_{k^*}}}\right)\right]^K \tag{4.11}$$

$$F_{|\hat{h}_{SR_{k^*}}|^2}(x) = \sum_{k=0}^{k=K}\binom{K}{K}(-1)^k \exp\left(\frac{-xk}{\rho_s\hat{\Omega}_{SR_{k^*}}}\right) \tag{4.12}$$

$$F_{|\hat{h}_{SR_{k^*}}|^2}(x) = 1 - \sum_{k=1}^{k=K}\binom{K}{K}(-1)^{k-1} \exp\left(\frac{-xk}{\rho_s\hat{\Omega}_{SR_{k^*}}}\right) \tag{4.13}$$

First Phase: The received signals at both mobile users D_1 and D_2 are given by

$$y_{D_1} = \left(\hat{h}_{SD_1} + e_{SD_1}\right)\left(\sqrt{a_1 p_s}x_1 + \sqrt{a_2 p_s}x_2\right) + n_{D_1} \tag{4.14}$$

$$y_{D_2} = \left(\hat{h}_{SD_2} + e_{SD_2}\right)\left(\sqrt{a_1 p_s}x_1 + \sqrt{a_2 p_s}x_2\right) + n_{D_2} \tag{4.15}$$

where n_{D_1} and n_{D_2} are AWGN with zero mean and variance σ^2, $\hat{h}_{SD_1}$ and $\hat{h}_{SD_2}$ are channel estimates of the fading channel coefficients h_{SD_1} , h_{SD_2}, respectively, a_i is power coefficient for symbol x_i, ı=1,2, and p_s is transmission power at S. As user1 is far away from the base station compared to user2, we assume $a_1 \geq a_2$. Let e_{SD_1}, e_{SD_2} indicate channel estimation errors at user1 and user2, respectively. The variances of e_{SD_1}, e_{SD_1} are $\sigma^2_{e_{SD_1}}$ and $\sigma^2_{e_{SD_2}}$, respectively.

The received SINR at D_1 to detect its symbol x_1 is given by

$$\gamma_1 = \frac{a_1 p_s|\hat{h}_{SD_1}|^2}{a_2 p_s|\hat{h}_{SD_1}|^2 + p_s\sigma^2_{e_{SD_1}} + \sigma^2} \tag{4.16}$$

After simplifying the above equation, we can rewrite it as follows

$$\gamma_1 = \frac{a_1 \rho_s|\hat{h}_{SD_1}|^2}{a_2 \rho_s|\hat{h}_{SD_1}|^2 + \rho_s\sigma^2_{e_{SD_1}} + 1} \tag{4.17}$$

The received SINR at D_2 to detect symbol x_1 is given by

$$\gamma_{1,2} = \frac{a_1 \rho_s|\hat{h}_{SD_2}|^2}{a_2 \rho_s|\hat{h}_{SD_2}|^2 + \rho_s\sigma^2_{e_{SD_2}} + 1} \tag{4.18}$$

The received SINR at D_2 to detect its symbol x_2 after SIC is given by

$$\gamma_2 = \frac{a_2 \rho_s |\hat{h}_{SD_2}|^2}{a_1 \beta_{SD_2} \rho_s |\hat{h}_{SD_2}|^2 + \rho_s \sigma^2_{e_{SD_2}} + 1} \tag{4.19}$$

where β_{SD_2} represents the level of residual interference due to imperfect SIC at D_2

Energy Harvesting Phase: The received signal at selected relay k^* from S during sub-block time αT is

$$y_{R_{k^*}} = \left(\hat{h}_{SR_{k^*}} + e_{SR_{k^*}}\right)\left(\sqrt{a_1 p_s} x_1 + \sqrt{a_2 p_s} x_2\right) + n_{R_{k^*}} \tag{4.20}$$

where $n_{R_{k^*}}$ represents AWGN at relay k^* having zero mean and variance σ^2, $\hat{h}_{SR_{k^*}}$ is estimated channel coefficient of $h_{SR_{k^*}}$, $e_{SR_{k^*}}$ is channel estimation error at selected relay and the variance of $e_{SR_{k^*}}$ is $\sigma^2_{e_{SR_{k^*}}}$.

The harvested energy is as follows:

$$E_H = \left(|\hat{h}_{SR_{k^*}}|^2 + \sigma^2_{e_{SR_{k^*}}}\right) p_s \alpha T \eta \tag{4.21}$$

where η is energy harvesting efficiency

The transmission power at R for forwarding the decoded signal to both users is

$$P_T = \frac{E_H}{(1-\alpha)T/2} \tag{4.22}$$

Decoding Phase: The received signal at selected relay k^* from S during sub-block time $(1-\alpha)\frac{T}{2}$ is

$$y_{R_{k^*}} = \left(\hat{h}_{SR_{k^*}} + e_{SR_{k^*}}\right)\left(\sqrt{a_1 p_s} x_1 + \sqrt{a_2 p_s} x_2\right) + n_{R_{k^*}} \tag{4.23}$$

The received SINR at R_{k^*} to detect symbol x_1 is given by

$$\gamma_{R,1} = \frac{a_1 \rho_s |\hat{h}_{SR_{k^*}}|^2}{a_2 \rho_s |\hat{h}_{SR_{k^*}}|^2 + \rho_s \sigma^2_{e_{SR_{k^*}}} + 1} \tag{4.24}$$

The received SINR at R_{k^*} to detect symbol x_2 after SIC is given by

$$\gamma_{R,2} = \frac{a_2 \rho_s |\hat{h}_{SR_{k^*}}|^2}{a_1 \beta_{SR_{k^*}} \rho_s |\hat{h}_{SR_{k^*}}|^2 + \rho_s \sigma^2_{e_{SR_{k^*}}} + 1} \tag{4.25}$$

where $\beta_{SR_{k^*}}$ represents the level of residual interference due to imperfect SIC at R_{k^*}

Second Phase: The received signal at D_1 and D_2 in the second phase can be expressed as

$$y_1^{DF} = \left(\hat{h}_{R_{k^*}D_1} + e_{R_{k^*}D_1}\right)\left(\sqrt{a_1 P_T} x_1 + \sqrt{a_2 P_T} x_2\right) + n_1 \tag{4.26}$$

$$y_2^{DF} = \left(\hat{h}_{R_{k^*}D_2} + e_{R_{k^*}D_2}\right)\left(\sqrt{a_1 P_T} x_1 + \sqrt{a_2 P_T} x_2\right) + n_2 \tag{4.27}$$

where n_1 and n_2 represent the AWGN at D_1 and D_2 with zero mean and variance σ^2, transmission power at relay is P_T, $\hat{h}_{R_{k^*}D_1}$ and $\hat{h}_{R_{k^*}D_2}$ are channel estimates of the fading channel coefficients $h_{R_{k^*}D_1}$

and $h_{R_{k^*}D_2}$, respectively, $e_{R_{k^*}D_1}$ and $e_{R_{k^*}D_2}$ are channel estimation errors at user1 and user2, respectively, and finally, the variances of $e_{R_{k^*}D_1}$ and $e_{R_{k^*}D_2}$ are $\sigma^2_{e_{R_{k^*}D_1}}$ and $\sigma^2_{e_{R_{k^*}D_2}}$, respectively.

The received SINR at D_1 to detect its symbol x_1 is given by

$$\gamma_1^{DF} = \frac{a_1 P_T |\hat{h}_{R_{k^*}D_1}|^2}{a_2 P_T |\hat{h}_{R_{k^*}D_1}|^2 + P_T \sigma^2_{e_{R_{k^*}D_1}} + \sigma^2} \tag{4.28}$$

$$\gamma_1^{DF} = \frac{a_1 \phi_E \rho_s |\hat{h}_{R_{k^*}D_1}|^2 \left(|\hat{h}_{SR_{k^*}}|^2 + \sigma^2_{e_{SR_{k^*}}}\right)}{a_2 \phi_E \rho_s |\hat{h}_{R_{k^*}D_1}|^2 \left(|\hat{h}_{SR_{k^*}}|^2 + \sigma^2_{e_{SR_{k^*}}}\right) + \sigma^2_{e_{R_{k^*}D_1}} \phi_E \rho_s \left(|\hat{h}_{SR_{k^*}}|^2 + \sigma^2_{e_{SR_{k^*}}}\right) + 1} \tag{4.29}$$

The received SINR at D_2 to detect symbol x_1 is given by

$$\gamma_{1,2}^{DF} = \frac{a_1 P_T |\hat{h}_{R_{k^*}D_2}|^2}{a_2 P_T |\hat{h}_{R_{k^*}D_2}|^2 + P_T \sigma^2_{e_{R_{k^*}D_2}} + \sigma^2} \tag{4.30}$$

After, substituting (4.22) in (4.30), we get

$$\gamma_{1,2}^{DF} = \frac{a_1 \phi_E \rho_s |\hat{h}_{R_{k^*}D_2}|^2 \left(|\hat{h}_{SR_{k^*}}|^2 + \sigma^2_{e_{SR_{k^*}}}\right)}{a_2 \phi_E \rho_s |\hat{h}_{R_{k^*}D_2}|^2 \left(|\hat{h}_{SR_{k^*}}|^2 + \sigma^2_{e_{SR_{k^*}}}\right) + \sigma^2_{e_{R_{k^*}D_2}} \phi_E \rho_s \left(|\hat{h}_{SR_{k^*}}|^2 + \sigma^2_{e_{SR_{k^*}}}\right) + 1} \tag{4.31}$$

The received SINR at D_2 to detect its symbol x_2 after SIC is given by

$$\gamma_2^{DF} = \frac{a_2 \phi_E \rho_s |\hat{h}_{R_{k^*}D_2}|^2 \left(|\hat{h}_{SR_{k^*}}|^2 + \sigma^2_{e_{SR_{k^*}}}\right)}{a_1 \beta_{R_{k^*}D_2} \phi_E \rho_s |\hat{h}_{R_{k^*}D_2}|^2 \left(|\hat{h}_{SR_{k^*}}|^2 + \sigma^2_{e_{SR_{k^*}}}\right) + \sigma^2_{e_{R_{k^*}D_2}} \phi_E \rho_s \left(|\hat{h}_{SR_{k^*}}|^2 + \sigma^2_{e_{SR_{k^*}}}\right) + 1} \tag{4.32}$$

where $\beta_{R_{k^*}D_2}$ represents the level of residual interference due to imperfect SIC at D_2

4.4 Performance Analysis

4.4.1 Outage Probability Analysis of user1

The outage probability of the D_1 is given by

$$P_1 = P\left(\max\left(\gamma_{SD_1}, \gamma_{R_{k^*}D_1}\right) < \gamma_{th}\right) \tag{4.33}$$

where, γ_{th} is SINR threshold

After simplifying the above equation, we can rewrite it as follows

$$P_1 = P\left(\gamma_1 < \gamma_{th}\right) P\left(\gamma_{R,1} < \gamma_{th} \cup \gamma_{R,2} < \gamma_{th} \cup \gamma_1^{DF} < \gamma_{th}\right) \tag{4.34}$$

Further, simplifying the above equation, we can rewrite it as follows

$$P_1 = P\left(\gamma_1 < \gamma_{th}\right)\left(1 - P\left(\gamma_{R,1} > \gamma_{th} \cap \gamma_{R,2} > \gamma_{th} \cap \gamma_1^{DF} > \gamma_{th}\right)\right) \tag{4.35}$$

After, substituting (4.17), (4.24), (4.29) in (4.35), we get

$$\mathrm{P}_1 = P\left[|\hat{h}_{SD_1}|^2 < \psi_1\right]\left[1 - P\left(|\hat{h}_{SR_{k^*}}|^2 > \psi_2 \cap |\hat{h}_{R_{k^*}D_1}|^2 > \frac{\gamma_{th}\left(\sigma^2_{e_{R_{k^*}D_1}}\phi_E\rho_s\left(|\hat{h}_{SR_{k^*}}|^2+\sigma^2_{e_{SR_{k^*}}}\right)+1\right)}{\left(|\hat{h}_{SR_{k^*}}|^2+\sigma^2_{e_{SR_{k^*}}}\right)(a_1-a_2\gamma_{th})\phi_E\rho_s}\right)\right]$$

$$where, \psi_1 = \frac{\gamma_{th}\left(1+\sigma^2_{e_{SD_1}}\rho_s\right)}{(a_1-a_2\gamma_{th})\rho_s},\ \ \psi_2 = \max\left(\frac{\gamma_{th}}{(a_1-a_2\gamma_{th})}, \frac{\gamma_{th}}{(a_2-a_1\beta_{SR_{k^*}}\gamma_{th})}\right)\left(\frac{1}{\rho_s}+\sigma^2 e_{e_{SR_{k^*}}}\right) \tag{4.36}$$

After, substituting (4.2), (4.13), (4.4) in above equation, we get

$$P_1 = \left[1-\exp\left(\frac{-\psi_1}{\hat{\Omega}_{SD_1}}\right)\right]\left[1-\sum_{k=1}^{k=K}\binom{K}{k}(-1)^{(k-1)}\left(\frac{k}{\hat{\Omega}_{SR_{k^*}}}\right)\exp\left(\frac{\sigma^2_{e_{SR_{k^*}}}k}{\hat{\Omega}_{SR_{k^*}}}\right)\right.$$
$$\left.\times\exp\left(\frac{-\gamma_{th}\sigma^2_{e_{R_{k^*}D_1}}}{(a_1-a_2\gamma_{th})\hat{\Omega}_{R_kD_1}}\right)\int_{\psi_2-\sigma^2_{e_{SR_{k^*}}}}^{\infty}\exp\left(\frac{-\tau'}{x\hat{\Omega}_{R_{k^*}D_1}}\right)\exp\left(\frac{-xk}{\hat{\Omega}_{SR_{k^*}}}\right)dx\right] \tag{4.37}$$

The integral $\int_{\psi_2-\sigma^2_{e_{SR_{k^*}}}}^{\infty}\exp\left(\frac{-\tau'}{x\hat{\Omega}_{R_{k^*}D_1}}\right)\exp\left(\frac{-xk}{\hat{\Omega}_{SR_{k^*}}}\right)dx$ can be solved by using Chebyshev gauss quadrature and by 1^{st} order modified Bessel function of the second kind [8, Eq. (3.324.1)].

By using Chebyshev gauss quadrature and first-order modified Bessel function of the second kind, the above equation can be rewritten as follows

$$P_1 \approx \left[1-\exp\left(\frac{-\psi_1}{\hat{\Omega}_{SD_1}}\right)\right]\left[1-\sum_{k=1}^{k=K}\binom{K}{k}(-1)^{(k-1)}\left(\frac{k}{\hat{\Omega}_{SR_{k^*}}}\right)\exp\left(\frac{\sigma^2_{e_{SR_{k^*}}}k}{\hat{\Omega}_{SR_{k^*}}}\right)\right.$$
$$\times\exp\left(\frac{-\gamma_{th}\sigma^2_{e_{R_{k^*}D_1}}}{(a_1-a_2\gamma_{th})\hat{\Omega}_{R_kD_1}}\right)\left[2\sqrt{\frac{\tau'\hat{\Omega}_{SR_{k^*}}}{k\hat{\Omega}_{R_{k^*}D_1}}}K_1\left(2\sqrt{\frac{\tau' k}{\hat{\Omega}_{SR_{k^*}}\hat{\Omega}_{R_{k^*}D_1}}}\right)-\right.$$
$$\times\sum_{i=1}^{S}W_i\sqrt{1-t_{i^2}}\exp\left(\frac{-\tau' 2}{(t_i+1)\left(\psi_2-\sigma^2_{e_{SR_{k^*}}}\right)\hat{\Omega}_{R_{k^*}D_1}}\right)$$
$$\left.\left.\times\exp\left(\frac{-(t_i+1)\left(\psi_2-\sigma^2_{e_{SR_{k^*}}}\right)k}{2\hat{\Omega}_{SR_{k^*}}}\right)\right]\right] \tag{4.38}$$

where $K_1(.)$ represents the first-order modified Bessel function of the second kind. [**gradshteyn2007**], $W_i = \pi/S$, $t_i = \cos\left(\frac{2i-1}{2S}\pi\right)$

4.4.2 Outage Probability Analysis of user2

The outage probability of the D_2 is given by

$$P_2 = P\left(\max\left(\gamma_{SD_2}, \gamma_{R_{k^*}D_2}\right) < \gamma_{th}\right) \tag{4.39}$$

$$P_2 = P\left(\gamma_{1,2} < \gamma_{th} \cup \gamma_2 < \gamma_{th}\right)P\left(\gamma_{R,1} < \gamma_{th} \cup \gamma_{R,2} < \gamma_{th} \cup \gamma_1^{DF} < \gamma_{th} \cup \gamma_{1,2}^{DF} < \gamma_{th}\right) \tag{4.40}$$

After simplifying the above equation, we can rewrite it as follows

$$P_2 = \left(1-P\left(\gamma_{1.2} > \gamma_{th} \cap \gamma_2 > \gamma_{th}\right)\right)\left(1-P\left(\gamma_{R,1} > \gamma_{th} \cap \gamma_{R,2} > \gamma_{th} \cap \gamma_1^{DF} > \gamma_{th} \cap \gamma_{1,2}^{DF} > \gamma_{th}\right)\right) \tag{4.41}$$

After, substituting (4.18), (4.19) (4.24), (4.25), (4.31), (4.32) in (4.41), we get

$$\mathrm{P}_2 = \left[1 - P\left(|\hat{h}_{SD_2}|^2 > \psi_3\right)\right]\left[1 - P\left(|\hat{h}_{SR_{k^*}}|^2 > \psi_2 \cap |\hat{h}_{R_{k^*}D_2}|^2 > \frac{\gamma_{th}\left(\sigma^2_{e_{R_{k^*}D_1}}\phi_E\rho_s\left(|\hat{h}_{SR_{k^*}}|^2 + \sigma^2_{e_{SR_{k^*}}}\right)+1\right)}{\left(|\hat{h}_{SR_{k^*}}|^2 + \sigma^2_{e_{SR_{k^*}}}\right)(a_1 - a_2\gamma_{th})\phi_E\rho_s}\right)\right]$$

$$\text{where } \psi_3 = \max\left(\frac{\gamma_{th}}{(a_1 - a_2\gamma_{th})}, \frac{\gamma_{th}}{(a_2 - a_1\beta_{SD_2}\gamma_{th})}\right)\left(\frac{1}{\rho_s} + \sigma^2_{e_{SD_2}}\rho_s\right) \tag{4.42}$$

$$\theta'' = \max\left(\frac{\gamma_{th}}{(a_1 - a_2\gamma_{th})\psi_E\rho_s}, \frac{\gamma_{th}}{(a_2 - a_1\beta_{R_{k^*}D_2}\gamma_{th})\psi_E\rho_s}\right) \tag{4.43}$$

After, substituting (4.2), (4.13), (4.4) in above equation, we get

$$P_2 = \left[1 - \exp\left(\frac{-\psi_3}{\hat{\Omega}_{SD_2}}\right)\right]\left[1 - \sum_{k=1}^{k=K}\binom{K}{k}(-1)^{(k-1)}\left(\frac{k}{\hat{\Omega}_{SR_{k^*}}}\right)\exp\left(\frac{\sigma^2_{e_{SR_{k^*}}}k}{\hat{\Omega}_{SR_{k^*}}}\right)\right.$$
$$\left.\times\exp\left(\frac{-\theta''\psi_E\rho_s\sigma^2_{e_{R_{k^*}D_2}}}{\hat{\Omega}_{R_kD_2}}\right)\int_{\psi_2-\sigma^2_{e_{SR_{k^*}}}}^{\infty}\exp\left(\frac{-\theta''}{x\hat{\Omega}_{R_{k^*}D_2}}\right)\exp\left(\frac{-xk}{\hat{\Omega}_{SR_{k^*}}}\right)dx\right] \tag{4.44}$$

The integral $\int_{\psi_2-\sigma^2_{e_{SR_{k^*}}}}^{\infty}\exp\left(\frac{-\theta''}{x\Omega_{R_{k^*}D_1}}\right)\exp\left(\frac{-xk}{\Omega_{SR_{k^*}}}\right)dx$ can be solved by using Chebyshev gauss quadrature and by 1st order modified Bessel function of the second kind[8, Eq. (3.324.1)].

By using Chebyshev gauss quadrature and first-order modified Bessel function of the second kind, the above equation can be rewritten as follows

$$P_2 \approx \left[1 - \exp\left(\frac{-\psi_3}{\hat{\Omega}_{SD_2}}\right)\right]\left[1 - \sum_{k=1}^{k=K}\binom{K}{k}(-1)^{(k-1)}\left(\frac{k}{\hat{\Omega}_{SR_{k^*}}}\right)\exp\left(\frac{\sigma^2_{e_{SR_{k^*}}}k}{\hat{\Omega}_{SR_{k^*}}}\right)\right.$$
$$\times\exp\left(\frac{-\theta''\psi_E\rho_s\sigma^2_{e_{R_{k^*}D_2}}}{\hat{\Omega}_{R_kD_2}}\right)\left[2\sqrt{\frac{\theta''\hat{\Omega}_{SR_{k^*}}}{k\hat{\Omega}_{R_{k^*}D_2}}}K_1\left(2\sqrt{\frac{\theta''k}{\hat{\Omega}_{SR_{k^*}}\hat{\Omega}_{R_{k^*}D_2}}}\right) - \right.$$
$$\times\sum_{i=1}^{S}W_i\sqrt{1-t_{i^2}}\exp\left(\frac{-\theta''2}{(t_i+1)\left(\psi_2 - \sigma^2_{e_{SR_{k^*}}}\right)\hat{\Omega}_{R_{k^*}D_2}}\right)$$
$$\left.\left.\times\exp\left(\frac{-(t_i+1)\left(\psi_2 - \sigma^2_{e_{SR_{k^*}}}\right)k}{2\hat{\Omega}_{SR_{k^*}}}\right)\right]\right] \tag{4.45}$$

4.4.3 Ergodic Capacity Analysis of user1

The ergodic capacity of the user1 is given by

$$C_1 = E\left[\frac{1}{2}log_2(1+Z_1)\right] \tag{4.46}$$

where W_1 is a random variable and W_1 = max $\left(\gamma_1, \min\left(\gamma_{R,1}, \gamma_1^{DF}\right)\right)$

$$C_1 = \frac{1}{2\ln(2)}\int_0^{\infty}\frac{1-F_{Z_1}(x)}{1+x}dx \tag{4.47}$$

$$\text{where, } F_{Z_1}(x) = P\left(\max\left(\gamma_1, \min\left(\gamma_{R,1}, \gamma_1^{DF}\right)\right)\right) \tag{4.48}$$

$$F_{Z_1}(x) = P\left(\gamma_1 < x \cap \min\left(\gamma_{R,1}, \gamma_1^{DF}\right) < x\right) \tag{4.49}$$

After simplifying the above equation, we can rewrite it as follows

$$F_{Z_1}(x) = P(\gamma_1 < x)\left(1 - P\left(\max\left(\gamma_{R,1}, \gamma_1^{DF}\right) > x\right)\right) \tag{4.50}$$

After substituting (4.17), (4.31), (4.24) in (4.50), we get

$$\mathrm{F}_{Z_1}(x) = P\left(|\hat{h}_{SD_1}|^2 < \xi_1\right)\left(1 - P\left(|\hat{h}_{SR_{k^*}}|^2 > \xi_2 \cap |\hat{h}_{R_{k^*}D_1}|^2 > \mu\left(\sigma^2 e_{R_{k^*}D_1} + \frac{1}{\left(|\hat{h}_{SR_{k^*}}|^2 + \sigma^2_{e_{SR_{k^*}}}\right)\phi_E \rho_s}\right)\right)\right)$$

$$\text{where } \mu = \frac{x}{(a_1 - a_2 x)\rho_s}, \quad \xi_1 = \frac{x\left(1 + \sigma^2_{e_{SD_1}}\rho_s\right)}{(a_1 - a_2 x)\rho_s}, \quad \xi_2 = \frac{x\left(1 + \sigma^2_{e_{SR_{k^*}}}\rho_s\right)}{(a_1 - a_2 x)\rho_s} \tag{4.51}$$

After substituting (4.2), (4.13), (4.4) in above equation, we get

$$\begin{aligned} F_{Z_1}(x) = &\left[1 - \exp\left(\frac{-\xi_1}{\hat{\Omega}_{SD_1}}\right)\right]\left[1 - \sum_{k=1}^{k=K}\binom{K}{k}(-1)^{(k-1)}\left(\frac{k}{\hat{\Omega}_{SR_{k^*}}}\right)\right. \\ &\times \exp\left(\frac{\sigma^2_{e_{SR_{k^*}}}k}{\hat{\Omega}_{SR_{k^*}}}\right)\exp\left(\frac{-\rho_s \mu \sigma^2_{e_{R_{k^*}D_1}}}{\hat{\Omega}_{R_{k^*}D_1}}\right) \\ &\left.\times \int_{\xi_2 - \sigma^2_{e_{SR_{k^*}}}}^{\infty} \exp\left(\frac{-\mu}{y\phi_E \hat{\Omega}_{R_{k^*}D_1}}\right)\exp\left(\frac{-yk}{\hat{\Omega}_{SR_{k^*}}}\right)dy\right] \end{aligned} \tag{4.52}$$

The above equation is valid only if $x < \frac{a_1}{a_2}$

After substituting (4.52) in (4.47), we get

$$C_1 = \frac{1}{2\ln(2)}\int_0^{\frac{a_1}{a_2}} \frac{\mathscr{E}}{1+x}dx \tag{4.53}$$

$$\begin{aligned} \mathscr{E} = &\exp\left(\frac{-\xi_1}{\hat{\Omega}_{SD_1}}\right) + \left[1 - \exp\left(\frac{-\xi_1}{\hat{\Omega}_{SD_1}}\right)\right]\left[\sum_{k=1}^{k=K}\binom{K}{k}(-1)^{(k-1)}\left(\frac{k}{\hat{\Omega}_{SR_{k^*}}}\right)\right. \\ &\times \exp\left(\frac{\sigma^2_{e_{SR_{k^*}}}k}{\hat{\Omega}_{SR_{k^*}}}\right)\exp\left(\frac{-\rho_s \mu \sigma^2_{e_{R_{k^*}D_1}}}{\hat{\Omega}_{R_{k^*}D_1}}\right) \\ &\left.\times \int_{\xi_2 - \sigma^2_{e_{SR_{k^*}}}}^{\infty} \exp\left(\frac{-\mu}{y\phi_E \hat{\Omega}_{R_{k^*}D_1}}\right)\exp\left(\frac{-yk}{\hat{\Omega}_{SR_{k^*}}}\right)dy\right] \end{aligned} \tag{4.54}$$

4.4.4 Ergodic Capacity Analysis of user2

The ergodic capacity of the user2 is given by

$$C_2 = E\left[\frac{1}{2}log_2(1+Z_2)\right] \tag{4.55}$$

where Z_2 is a random variable and $Z_2 = \max\left(\gamma_2, \min\left(\gamma_{R,2}, \gamma_2^{DF}\right)\right)$

$$C_2 = \frac{1}{2\ln(2)} \int_0^\infty \frac{1 - F_{Z_2}(x)}{1+x} dx \tag{4.56}$$

$$\text{where } F_{Z_2}(x) = P\left(\max\left(\gamma_2, \min\left(\gamma_{R,2}, \gamma_2^{DF}\right)\right)\right) \tag{4.57}$$

$$F_{Z_2}(x) = P\left(\gamma_2 < x \cap \min\left(\gamma_{R,2}, \gamma_2^{DF}\right) < x\right) \tag{4.58}$$

After simplifying the above equation, we can rewrite it as follows

$$F_{Z_2}(x) = P\left(\gamma_2 < x\right)\left(1 - P\left(\max\left(\gamma_{R,2}, \gamma_2^{DF}\right) > x\right)\right) \tag{4.59}$$

After, substituting (4.19), (4.32), (4.25) in (4.59), we get

$$\mathrm{F}_{Z_2}(x) = P\left(|\hat{h}_{SD_2}|^2 < \xi_3\right)\left(1 - P\left(|\hat{h}_{SR_{k^*}}|^2 > \xi_4 \cap |\hat{h}_{R_{k^*}D_2}|^2 > \xi_5\left(\sigma^2 e_{R_{k^*}D_2} + \frac{1}{\left(|\hat{h}_{SR_{k^*}}|^2 + \sigma^2_{e_{SR_{k^*}}}\right)\phi_E \rho_s}\right)\right)\right)$$

$$\text{where} \quad \xi_3 = \frac{x\left(1 + \sigma^2_{e_{SD_2}}\rho_s\right)}{\left(a_2 - a_1\beta_{SD_2}x\right)\rho_s}, \quad \xi_4 = \frac{x\left(1 + \sigma^2_{e_{SR_{k^*}}}\rho_s\right)}{\left(a_2 - a_1\beta_{SR_{k^*}}x\right)\rho_s}, \quad \text{and} \ \ \xi_5 = \frac{x}{\left(a_2 - a_1\beta_{R_{k^*}D_2}x\right)\rho_s} \tag{4.60}$$

After, substituting (4.2), (4.13), (4.4) in above equation, we get

$$\begin{aligned} F_{Z_2}(x) = \left[1 - \exp\left(\frac{-\xi_3}{\hat{\Omega}_{SD_2}}\right)\right]\Bigg[1 - \sum_{k=1}^{k=K}\binom{K}{k}(-1)^{(k-1)}\left(\frac{k}{\hat{\Omega}_{SR_{k^*}}}\right) \\ \times \exp\left(\frac{\sigma^2_{e_{SR_{k^*}}}k}{\hat{\Omega}_{SR_{k^*}}}\right)\exp\left(\frac{-\xi_5\sigma^2_{e_{R_{k^*}D_2}}}{\hat{\Omega}_{R_{k^*}D_2}}\right) \\ \times \int_{\xi_4 - \sigma^2_{e_{SR_{k^*}}}}^{\infty} \exp\left(\frac{-\xi_5}{y\phi_E\hat{\Omega}_{R_{k^*}D_2}}\right)\exp\left(\frac{-yk}{\hat{\Omega}_{SR_{k^*}}}\right)dy\Bigg] \end{aligned} \tag{4.61}$$

The above equation is valid if $x < \frac{a_2}{a_1\beta_{SD_2}}$

After, substituting (4.61) in (4.56), we can rewrite it as follows

$$C_2 = \frac{1}{2\ln(2)} \int_0^{\frac{a_2}{a_1\beta_{SD_2}}} \frac{\mathscr{F}}{1+x} dx \tag{4.62}$$

$$\begin{aligned} \mathscr{F} = \exp\left(\frac{-\xi_3}{\hat{\Omega}_{SD_2}}\right) + \left[1 - \exp\left(\frac{-\xi_3}{\hat{\Omega}_{SD_2}}\right)\right]\Bigg[\sum_{k=1}^{k=K}\binom{K}{k}(-1)^{(k-1)}\left(\frac{k}{\hat{\Omega}_{SR_{k^*}}}\right) \\ \times \exp\left(\frac{\sigma^2_{e_{SR_{k^*}}}k}{\hat{\Omega}_{SR_{k^*}}}\right)\exp\left(\frac{-\xi_5\sigma^2_{e_{R_{k^*}D_2}}}{\hat{\Omega}_{R_{k^*}D_2}}\right) \\ \times \int_{\xi_4 - \sigma^2_{e_{SR_{k^*}}}}^{\infty} \exp\left(\frac{-\xi_5}{y\phi_E\hat{\Omega}_{R_{k^*}D_2}}\right)\exp\left(\frac{-yk}{\hat{\Omega}_{SR_{k^*}}}\right)dy\Bigg] \end{aligned} \tag{4.63}$$

4.5 Numerical Results and Discussions

In this section, we will analyze the derived closed-form expressions. We also demonstrate the effects of various parameters on outage probability, overall system throughput, ergodic capacity for the proposed system model. For numerical investigation, we set $a_1 = 0.7$, $a_2 = 0.3$, γ_{th} = 2 dB, $n_p = 4$, $R_1 = 1.5, R_2 = 1.5$, $\Omega_{SD_1} = (1)^{-4}$, $\Omega_{SD_2} = (0.75)^{-4}$, $\Omega_{SR_{k^*}} = (0.5)^{-4}$, $\Omega_{R_{k^*}D_1} = (0.5)^{-4}$, and $\Omega_{R_{k^*}D_2} = (0.25)^{-4}$, =0.7, $\eta = 0.8$, S = 4.

For simplicity assume $\beta_{SD_2} = \beta_{SR_{k^*}} = \beta_{R_{k^*}D_2} = \beta$ and $\sigma^2_{e_{SD_1}} = \sigma^2_{e_{SD_2}} = \sigma^2_{e_{SR_{k^*}}} = \sigma^2_{e_{R_{k^*}D_1}} = \sigma^2_{e_{R_{k^*}D_2}} = \sigma^2_e$.

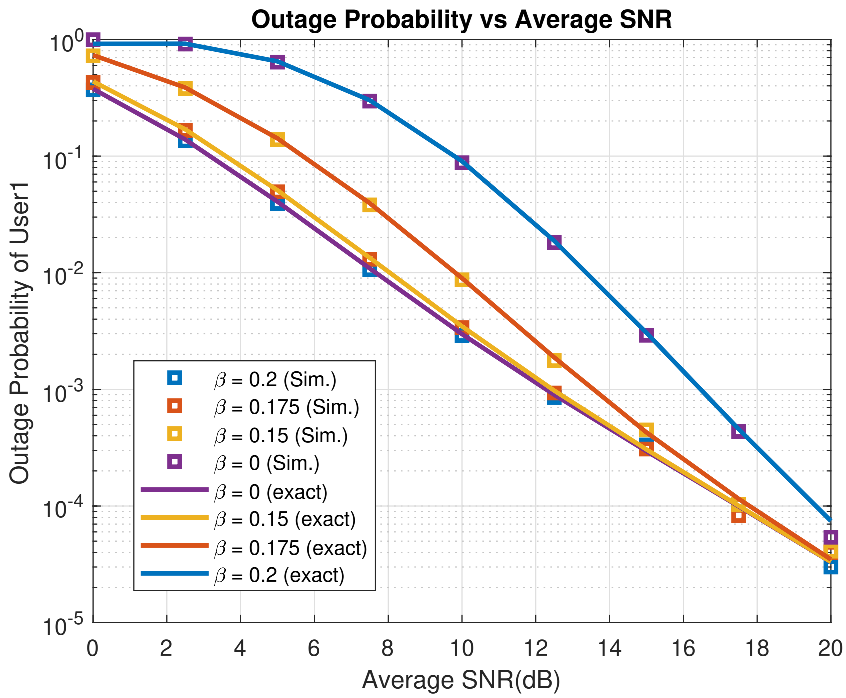

Figure 4.1: Outage Probability vs. Average SNR of user1 for different values of β. $\sigma_e^2 = 0$

Figure 4.1 shows the effect of value of β on the outage probability of the user1. From the plot, we can observe that with the decrease in the value of β, the outage performance improves. This is because of the residual interference due to imperfect SIC decreases with decrease in β. For user1 to achieve the outage probability of 10^{-2}, the SNR required for the system with β = 0, β =0.15, β = 0.175, and β = 2 are 7.8 dB, 8 dB, 10 dB, 13 dB, respectively. So, the SNR gain achieved by the system with β =0.15, β = 0.175, and β = 2 w.r.t system with β = 0, are 0.2 dB, 2.2 dB, 5.2 dB respectively. So, it has been inferred that in order to achieve the same outage performance that is obtained by the system having perfect SIC, the system having imperfect SIC have to transmit the signal with more power. When SNR increases, the outage probability tends to decrease. It is because, as SNR increases, the signal becomes much stronger than the noise.

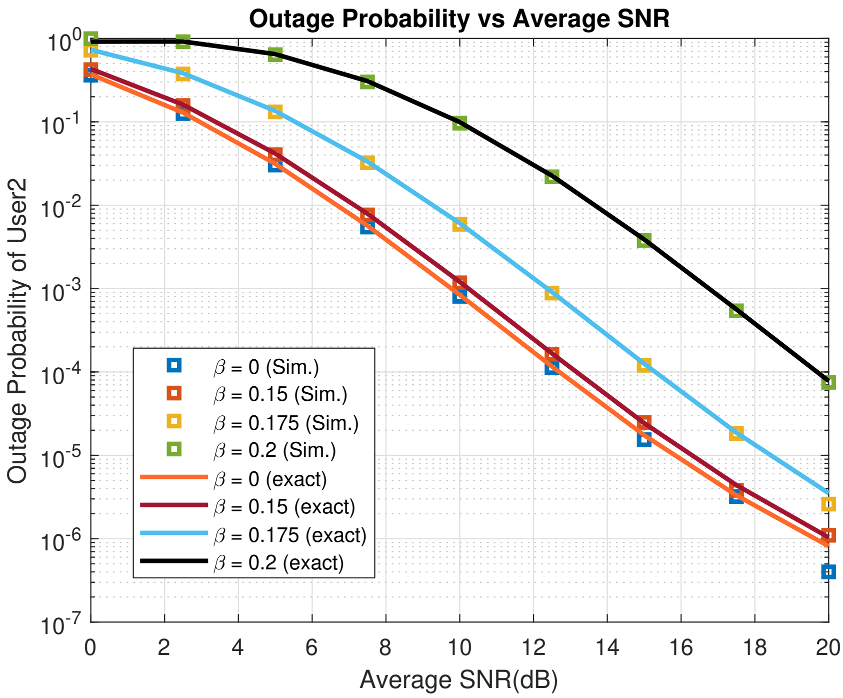

Figure 4.2: Outage Probability vs. Average SNR of user2 for different values of β. $\sigma_e^2 = 0$

Figure 4.2 shows the effect of value of β on the outage probability of the user2. From the plot, we can observe that with the decrease in the value of β, the outage performance improves this is because of the residual interference due to imperfect SIC decreases with decrease in β. For user2 to achieve the outage probability of 10^{-2}, the SNR required for the system with β = 0, β =0.15, β = 0.175, and β = 2 are 6.5 dB, 7 dB, 9 dB, 13.5 dB, respectively. So, the SNR gain achieved by the system with β =0.5, β = 2.5, and β = 2 w.r.t system with β = 0, are 4.5 dB, 6.5 dB, 7 dB respectively. So, it has been inferred that in order to achieve the same outage performance that is obtained by the system having perfect SIC, the system having imperfect SIC have to transmit the signal with more power.

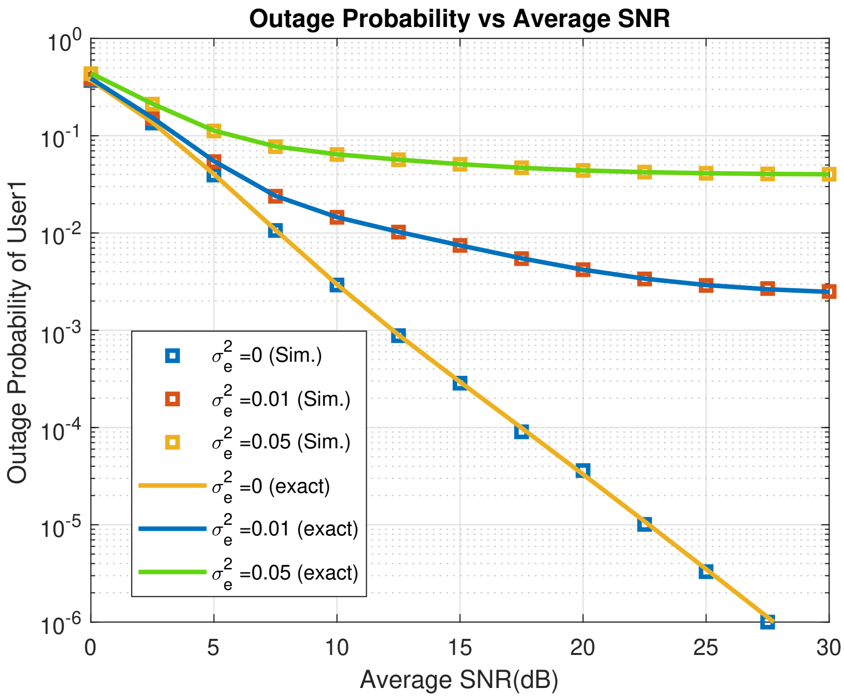

Figure 4.3: Outage Probability vs. Average SNR of user1 for different values of σ_e^2. $\beta = 0$

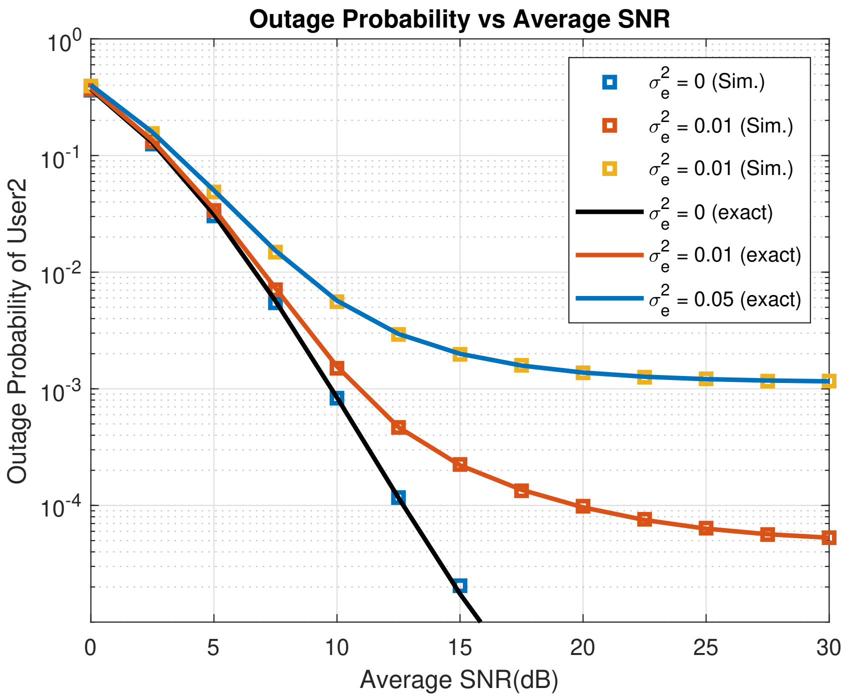

Figure 4.4: Outage Probability vs. Average SNR of user2 for different values of σ_e^2. $\beta = 0$

Figure 4.3 and Figure 4.4 show the effect of value of σ_e^2 on the outage probability of the user1 and user2 respectively. From the plot, we can observe that with the increase in the value of σ_e^2, the outage performance improves and this is because of the decrease in channel estimate errors. For both user1 and user2, with an increase in the SNR value, the outage performance for the system with perfect CSI improves. However, if the system has hardware impairments, i.e., imperfect CSI, the outage floor is achieved at a high SNR region. The outage floor exists if there are any hardware impairments in the system.

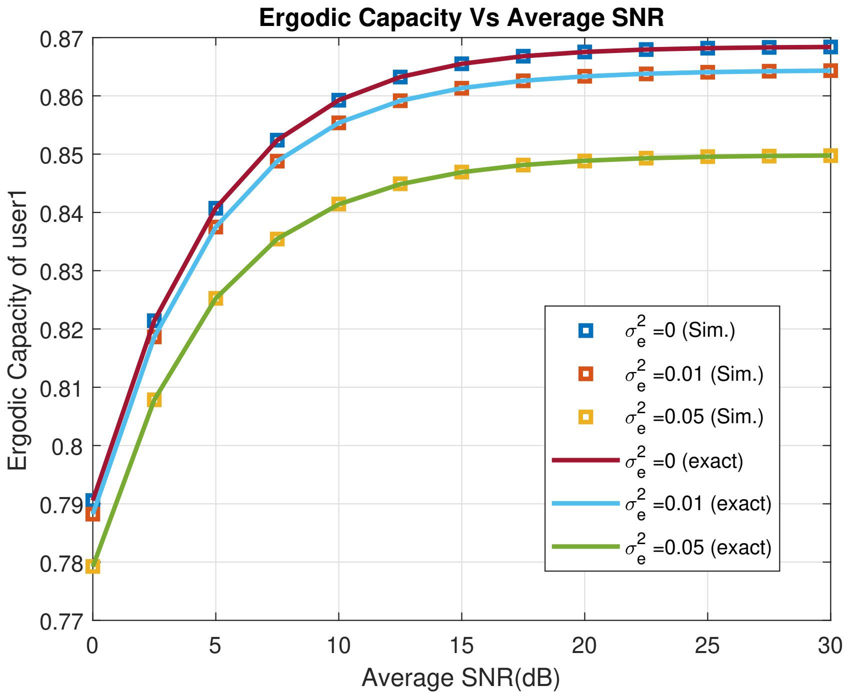

Figure 4.5: Ergodic Capacity vs. Average SNR of user1 for different values of σ_e^2. $\beta = 0$

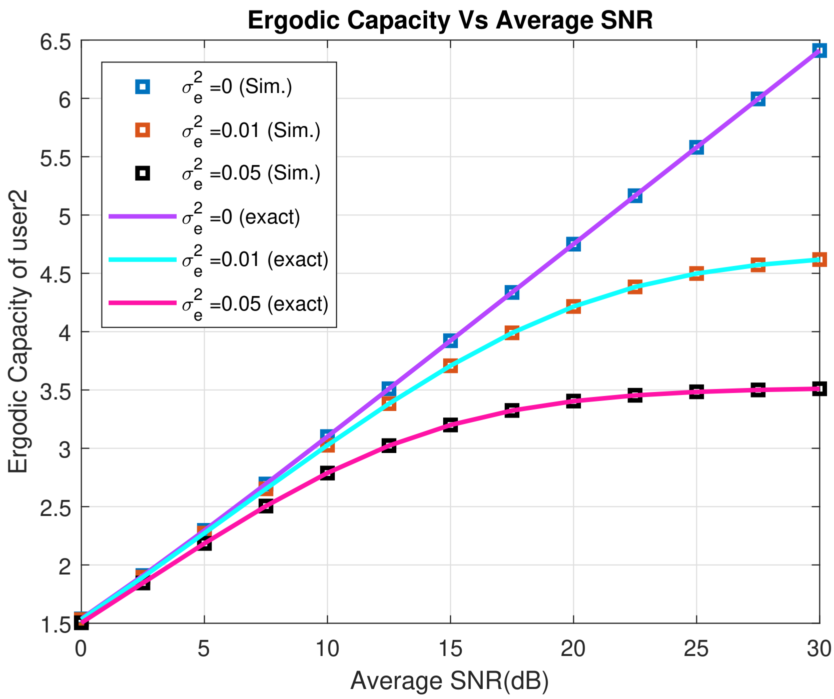

Figure 4.6: Ergodic Capacity vs. Average SNR of user2 for different values of σ_e^2. $\beta = 0$

Figure 4.5 and Figure 4.6 show the effect of value of σ_e^2 on the ergodic capacity of the user1 and user2 respectively. For both user1 and user2, with an increase in the value of the σ_e^2, ergodic capacity suffers a rate loss and approaches ceiling at high SNR region. For user1 with an increase in σ_e^2 value from 0 to 0.05, the ergodic capacity reduces by 0.02 bps/Hz at the high SNR region. For user2 with an increase in σ_e^2 value from 0 to 0.05, the ergodic capacity reduces by 3 bps/Hz at the high SNR region. For user1, the ergodic capacity saturates at the high SNR. It is because user1 decodes its signal by considering the user2 signal as noise. For user2, the ergodic capacity increases linearly with SNR. It is because while decoding its signal, user2 has no interference with the user1 signal.

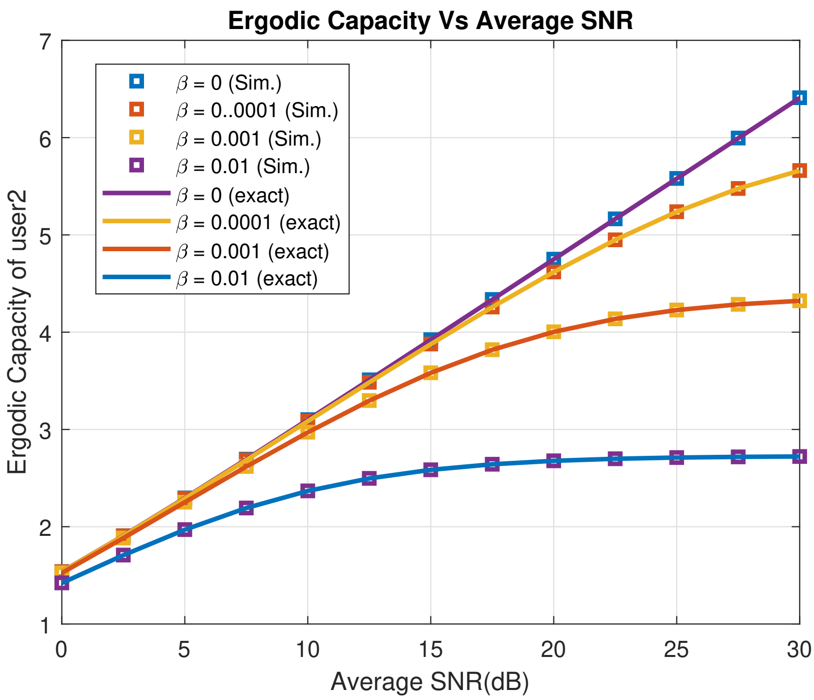

Figure 4.7: Ergodic Capacity vs. Average SNR of user2 for different values of β. $\sigma_e^2 = 0$

Figure 4.7 shows the effect of value of β on the ergodic capacity of the user2. Ergodic capacity increases with a decrease in the value of β. The ergodic capacity suffers a rate loss and approaches ceiling at high SNR region if the system was having imperfect SIC. With an increase in beta value from 0 to 0.01, the ergodic capacity reduced by 3.5 bps/Hz at the high SNR region.

4.6 Conclusions

In this chapter, the performance analysis of the SWIPT-enabled cooperative NOMA system model for DF networks with imperfect CSI and SIC is carried out by deriving the exact outage probability and ergodic capacity expressions in closed-from over Rayleigh fading channels. Furthermore, closed-form expressions for performance metrics such as outage probability and ergodic capacity of the proposed system model are implemented in MATLAB. From simulation results, it is observed that the outage performance of the proposed system model for both users improve with the decrease in value of β and $\sigma_e^2 = 0$. If the system has hardware impairments, i.e., imperfect CSI, the outage floor is achieved at a high SNR region. The ergodic capacity suffers a rate loss and approaches ceiling at high SNR region if the system had imperfect SIC. Also, it is observed that ergodic capacity for user1 saturates at high SNR while ergodic capacity for user2 proportionally increases with SNR. It is inferred from the simulation results that the ergodic capacity of both users increases with an decrease in value of β and $\sigma_e^2 = 0$. Finally, the simulated outage probability and ergodic capacity values obtained from Monte Carlo simulations agree well with the theoretical outage probability and ergodic capacity values. Therefore, the derived expressions are validated using Monte-Carlo simulations as well.

Chapter 5

Conclusions and Future Works

This thesis examines the performance of the following three system models: cooperative NOMA for DF relay networks, SWIPT-enabled cooperative NOMA for DF networks, and SWIPT-enabled cooperative NOMA for DF networks with imperfect SIC and CSI. The analytical framework in this thesis has been carried out over Rayleigh fading channels. The derived closed-form expressions for performance metrics are validated by Monte-Carlo-based simulations.

5.1 Conclusions

In chapter 2, we investigated the performance of the proposed system model of NOMA with partial relay selection for DF Relay Networks. The closed-form expressions for performance metrics such as outage probability, ergodic capacity, and overall system throughput of the proposed system model are derived and implemented in MATLAB. Numerical results elucidated the effect of the number of relays on the performance of the proposed system. Our proposed system outperforms the system without relay in terms of outage probability and system throughput.

In chapter 3, we investigated the SWIPT-enabled cooperative NOMA system model for DF networks. The closed-form expressions for performance metrics such as outage probability, ergodic capacity, energy efficiency, and overall system throughput of the proposed system model are derived and implemented in MATLAB. From the numerical results, we have observed the effect of target rate on the energy efficiency and observed the impact of the number of relays on the system performance.

In chapter 4, we investigated the SWIPT-enabled cooperative NOMA system model for DF networks with imperfect CSI and SIC. The closed-form expressions for performance metrics such as outage probability, ergodic capacity, and overall system throughput of the proposed system model are derived and implemented in MATLAB. From the numerical results, the effect of hardware impairments like channel estimate error and level of residual error on the performance of the system are investigated.

5.2 Future Works

The scope for the future work can be summarized as follows:

- The performance of the SWIPT-enabled cooperative NOMA system model is carried out by assuming a linear energy harvesting model. However, in practical scenarios, linear energy harvesting models are not possible. Hence, performance analysis was carried out by considered non-energy harvesting models.

- The performance of all proposed system models is carried over the Rayleigh fading channel model. Hence, performance analysis is carried out over generalized fading channel models.

- Investigation on the performance of SWIPT-enabled cooperative NOMA with incremental relaying has not been found in the literature. Hence, the performance analysis of the SWIPT-enabled cooperative NOMA system with incremental relaying is one of the key areas which can be thoroughly explored.

- In order to make our proposed system model more spectral efficient, FD technique can be employed. So, performance analysis can be carried out by considering the FD mode at relays.

- We will also discuss the implications of physical layer security in terms of the probability of secrecy capacity and secrecy outage probability. The average secrecy capacity and secrecy outage are the important secrecy performance metrics to evaluate the security performance over active and passive eavesdropping, respectively. We believe that the secrecy performance results will open a new way of designing secure SWIPT-enabled NOMA networks.

Bibliography

[1] Muhammad Waseem Akhtar et al. "STBC-Aided Cooperative NOMA With Timing Offsets, Imperfect Successive Interference Cancellation, and Imperfect Channel State Information". In: *IEEE Transactions on Vehicular Technology* 69.10 (2020), pp. 11712–11727. DOI: 10.1109/TVT.2020.3017249.

[2] Mahmoud Aldababsa et al. "A Tutorial on Nonorthogonal Multiple Access for 5G and Beyond". In: *Wireless Communications and Mobile Computing* 2018 (June 2018), pp. 1–24. ISSN: 1530-8677. DOI: 10.1155/2018/9713450. URL: http://dx.doi.org/10.1155/2018/9713450.

[3] A. Bletsas et al. "A simple Cooperative diversity method based on network path selection". In: *IEEE Journal on Selected Areas in Communications* 24.3 (2006), pp. 659–672. DOI: 10.1109/JSAC.2005.862417.

[4] Ishan Budhiraja et al. "A Systematic Review on NOMA Variants for 5G and Beyond". In: *IEEE Access* (2021), pp. 1–1. DOI: 10.1109/ACCESS.2021.3081601.

[5] Zhiguo Ding et al. "A Survey on Non-Orthogonal Multiple Access for 5G Networks: Research Challenges and Future Trends". In: *IEEE Journal on Selected Areas in Communications* 35.10 (2017), pp. 2181–2195. DOI: 10.1109/JSAC.2017.2725519.

[6] Dinh-Thuan Do, Mojtaba Vaezi, and Thanh-Luan Nguyen. "Wireless Powered Cooperative Relaying Using NOMA with Imperfect CSI". In: *2018 IEEE Globecom Workshops (GC Wkshps)*. 2018, pp. 1–6. DOI: 10.1109/GLOCOMW.2018.8644154.

[7] Wei Duan et al. "Two-Stage Superposed Transmission for Cooperative NOMA Systems". In: *IEEE Access* 6 (2018), pp. 3920–3931. DOI: 10.1109/ACCESS.2017.2789193.

[8] I.S. Gradshteyn and I.M. Ryzhik. "Table of Integrals, Series, and Products". In: (2007). URL: http://fisica.ciens.ucv.ve/~svincenz/TISPISGIMR.pdf.

[9] Azar Hakimi et al. "Full-Duplex Non-Orthogonal Multiple Access Cooperative Spectrum-Sharing Networks With Non-Linear Energy Harvesting". In: *IEEE Transactions on Vehicular Technology* 69.10 (2020), pp. 10925–10936. DOI: 10.1109/TVT.2020.3000995.

[10] Ferdi Kara and Hakan Kaya. "Improved User Fairness in Decode-Forward Relaying Non-Orthogonal Multiple Access Schemes With Imperfect SIC and CSI". In: *IEEE Access* 8 (2020), pp. 97540–97556. DOI: 10.1109/ACCESS.2020.2997285.

[11] Sunyoung Lee, Daniel Benevides da Costa, and Trung Q. Duong. "Outage probability of non-orthogonal multiple access schemes with partial relay selection". In: *2016 IEEE 27th Annual International Symposium on Personal, Indoor, and Mobile Radio Communications (PIMRC)*. 2016, pp. 1–6. DOI: 10.1109/PIMRC.2016.7794655.

[12] Guoxin Li, Deepak Mishra, and Hai Jiang. "Cooperative NOMA With Incremental Relaying: Performance Analysis and Optimization". In: *IEEE Transactions on Vehicular Technology* 67.11 (2018), pp. 11291–11295. DOI: 10.1109/TVT.2018.2869531.

[13] Xingwang Li et al. "Joint Effects of Residual Hardware Impairments and Channel Estimation Errors on SWIPT Assisted Cooperative NOMA Networks". In: *IEEE Access* 7 (2019), pp. 135499–135513. DOI: 10.1109/ACCESS.2019.2942337.

[14] Hongwu Liu et al. "Decode-and-Forward Relaying for Cooperative NOMA Systems With Direct Links". In: *IEEE Transactions on Wireless Communications* 17.12 (2018), pp. 8077–8093. DOI: 10.1109/TWC.2018.2873999.

[15] Ali A. Nasir et al. "Relaying Protocols for Wireless Energy Harvesting and Information Processing". In: *IEEE Transactions on Wireless Communications* 12.7 (2013), pp. 3622–3636. DOI: 10.1109/TWC.2013.062413.122042.

[16] Kehinde O. Odeyemi and Pius A. Owolawi. "Performance Analysis of Cooperative NOMA with Partial Relay Selection under Outdated Channel Estimate". In: *2019 IEEE 2nd Wireless Africa Conference (WAC)*. 2019, pp. 1–5. DOI: 10.1109/AFRICA.2019.8843391.

[17] Huu Q. Tran, Ca V. Phan, and Quoc-Tuan Vien. "Power splitting versus time switching based cooperative relaying protocols for SWIPT in NOMA systems". In: *Physical Communication* 41 (2020), p. 101098. ISSN: 1874-4907. DOI: https://doi.org/10.1016/j.phycom.2020.101098. URL: https://www.sciencedirect.com/science/article/pii/S1874490720301749.

[18] Dawei Wang and Shaoyang Men. "Secure Energy Efficiency for NOMA Based Cognitive Radio Networks With Nonlinear Energy Harvesting". In: *IEEE Access* 6 (2018), pp. 62707–62716. DOI: 10.1109/ACCESS.2018.2876970.

[19] Zhenling Wang et al. "Performance Analysis of Cooperative NOMA Systems with Incremental Relaying". In: *Wireless Communications and Mobile Computing* 2020 (Mar. 2020), p. 4915638. ISSN: 1530-8669. DOI: 10.1155/2020/4915638. URL: https://doi.org/10.1155/2020/4915638.

[20] Zhongyu Wang, Tiejun Lv, and Weicai Li. "Energy Efficiency Maximization in Massive MIMO-NOMA Networks with Non-linear Energy Harvesting". In: *2021 IEEE Wireless Communications and Networking Conference (WCNC)*. 2021, pp. 1–6. DOI: 10.1109/WCNC49053.2021.9417389.

[21] Wei Wu et al. "Transceiver Design for Downlink SWIPT NOMA Systems With Cooperative Full-Duplex Relaying". In: *IEEE Access* 7 (2019), pp. 33464–33472. DOI: 10.1109/ACCESS.2019.2904734.

[22] Zhongwu Xiang, Xiaobing Tong, and Yueming Cai. "Secure transmission for NOMA systems with imperfect SIC". In: *China Communications* 17.11 (2020), pp. 67–78. DOI: 10.23919/JCC.2020.11.006.